

Status, Trends and Significance of Single Phase, Single and Coupled Natural Circulation Loops in Sustainable Energy Technologies – A Comprehensive Review

D. N. Elton*, U. C. Arunachala**

* Renewable Energy Center, Dept. of Mech. & Mfg. Engg., Manipal Institute of Technology, Manipal Academy of Higher Education, Manipal – 576104, Karnataka State, India

** Renewable Energy Center, Dept. of Mech. & Mfg. Engg., Manipal Institute of Technology, Manipal Academy of Higher Education, Manipal – 576104, Karnataka State, India

(nazareth.elton@gmail.com, arun.chandavar@manipal.edu)

‡Corresponding Author; U. C. Arunachala, Renewable Energy Center, Dept. of Mech. & Mfg. Engg., Manipal Institute of Technology, Manipal Academy of Higher Education, Manipal – 576104, Karnataka State, India, Tel: +91-820-2925461, arun.chandavar@manipal.edu

Received: 23.08.2021 Accepted:12.09.2021

Abstract- Researchers have made continuous efforts to understand the behavior of the natural circulation systems, their application, and the challenges involved in implementation. A large number of numerical, analytical, and experimental studies during recent years reflect the importance of passive technology. However, there is a dearth of systematic review of such studies based on geometry, loop fluid, and the intended application. Hence, the present review extensively focuses on thermal-hydraulic parameters in single-phase single and coupled loop natural circulation systems. Performance aspects like steady-state, transient, and stability criteria, including instability restraining techniques have been discussed. Even the importance of validating the numerical codes is highlighted. Since the coupled natural circulation loop finds major application in nuclear reactors as passive cooling systems, various configurations and fluid combinations intended are illustrated. As there is a dearth of experimental studies in the coupled loop, a preliminary analysis was done, which showed the efficacy of such a system. The review further revealed the scope for experimental studies along with numerical analysis of the single and coupled system, which can be linked to sustainable and renewable energy applications.

Keywords Steady-state and transient analysis, Instability, Coupled natural circulation systems, Decay heat removal system, Beam down solar plant.

1. Introduction

The natural circulation (NC) systems don't require any mechanical component for the fluid motion but need a channel or path to travel. In general, the combination of a heat source and heat sink along with connecting pipes is referred to as a natural circulation loop (NCL). Such density gradient-based flow systems are more reliable than forced systems as the fluid circulation mechanism is power-free. In particular, single-phase NCL (SPNCL) systems have extensive applications in industries such as solar thermal systems, nuclear reactors, electronics, transformers, etc. due to their inherent advantages.

NCLs are classified based on the orientation of the source and sink as horizontal heater horizontal cooler (HHHC), horizontal heater vertical cooler (HHVC), vertical heater horizontal cooler (VHHC), and vertical heater vertical cooler (VHVC) [1]. The heat source may be solar thermal, nuclear, or others and the sink can be an atmosphere (particularly in case of decay heat removal) or a heat source for the next NCL (in coupled natural circulation loop (CNCL)). The HHHC configuration suits the solar parabolic trough collector (PTC) as the heater may replace the receiver and the cooler is the process fluid based heat exchanger. The pressurized heavy water reactor (PHWR) has an HHVC configuration, where the vertical cooler would be the steam generator. With a

horizontal steam generator and vertical core, the Voda Voda energy reactor (VVER) would have a VHHC configuration and the VHVC combination is in the Pressurized water reactor (PWR) as both the core and the steam generator are vertically placed. Further, if such a loop is coupled at either the heat source or the heat sink, the system is known as CNCL, which can be in series, parallel, or a combination of both [1]. Here, the working fluid in each loop may be the same or different. Even the combination of single-phase and two-phase loops is possible.

The functioning of NCL/CNCL largely depends on the operating condition, geometry, and loop fluid. Hence the influence of those parameters on steady-state, transient, and stability behavior is the prime focus of every researcher. Although instability exists both in NCL and pumped system, the former is inherently less stable due to regenerative feedback in the NC process. Instability is undesirable as it may cause component vibration, flow oscillations, disturbance to control systems, and operational problems. Hence, for identification analytical, numerical or an experimental procedure is being used. However, an experimental approach is realistic and has always been the benchmark for other kinds of analyses. In this context, the current review focuses primarily on the experimental and validated analytical/numerical studies in SPNCL and CNCL. The earlier reviews are summarized in section 2 followed by recent developments in SPNCL in section 3. The advancements in CNCL have been discussed in the 4th section and the preliminary experimental analysis is briefed in section 5. At the end (section 6), the limitations of such analyses with scope for future studies have been quoted.

2. Appraisal of earlier reviews

A comprehensive review by Basu et al. [2] included the literature on SPNCL during 1980 – 2014, aiming at solar and nuclear applications. The key content of the review is the significance and inception of scaling philosophy, challenges and development in modeling techniques, progress in multi-dimensional system codes, and instability restraining techniques (including nanofluids). The economic and computational analysis of solar thermal systems and the role of liquid metals in the development of generation IV nuclear reactors were quoted as an upcoming field of research. Later, Sarkar et al. [3] have reviewed the application of super-critical fluids in NCLs and mentioned the dearth of experimental analysis. Notable interpretations were the proportionality of mass flow rate with power up to a certain limit followed by drop as in the case of two-phase NC systems, higher velocity and heat transfer coefficient of sCO₂ than water, and the influence of operating and geometric parameters on steady-state behavior. Due to the unique behavior of CO₂ in the sub-critical and super-critical regions, Nu correlations couldn't accurately predict the performance. Hence the lack of experimental data to predict the transient and stability behavior of sCO₂ was highlighted.

The research scope mentioned in earlier reviews has been addressed by many researchers during the past six years.

Hence the forthcoming sections are related to the review of SPNCL and CNCL studies.

3. Studies on natural circulation loop

The influence of fluid on the loop stability is significant. Hence water, nanofluid, sCO₂, and liquid metals have been exercised.

3.1. Water

The affinity of water led to large volume research by adopting various experimental techniques and computational tools.

The balance point (pressure gain and pressure drop) of NCL defines HTF mass flow rate, which includes the loop diameter. Hence, Vijayan et al. [4] have analyzed the effect of loop diameter (6 mm to 26.9 mm in HHHC) on the steady-state mass flow rate (Eq. (1)), as it has practical relevance in boiling water reactors, where single-phase NC exists during the heat-up phase. In general, with a large length and/or smaller diameter ($Lt/di > 300$), the loop tends to be stable [1]. Even the stability threshold dependence on operating procedure i.e., hysteresis phenomenon is observed by Elton et al. [5] in a larger diameter loop (38.3 mm), which had quite a different instability pattern (compared to [4]) due to diametral effect. Further, the proportionality of mass flow rate with loop height was also observed [4] and found a deviation of $\pm 30\%$ compared to the Vijayan correlation [6]. Hence the steady state Re was modified (Eq. 2) for a better agreement.

One of the most observed unstable conditions is during the start-up from rest, where the low flow near the walls shows a significant secondary circulation. Since the conventional constitutive laws (for forced systems) aren't appropriate here, Naveen et al. [7] have proposed the wall friction factor correlation for HHHC (Eq. 3), which can supersede the earlier erroneous correlations [8, 9]. It found good agreement with experimental data and even predicted well the transient condition for the instabilities in previous studies [4].

$$w = \left[\frac{2D^b \rho^2 \beta_T g A^{2-b} Q_h \Delta z}{\rho C_P \mu^b N_G} \right]^{1/3-b} \quad (1)$$

$$Re_{ss} = 0.9668 \left[\frac{Gr_m}{N_G} \right]^{2/3} \quad (2)$$

$$f = \begin{cases} f_L \left[1 + \left(f_T / f_L \right)^{6.4} \right]^{1/6.4} & \text{Horizontal pipes} \\ \left[16 / Re, 0.079 / Re^{0.25} \right] & \text{Vertical pipes} \end{cases} \quad (3)$$

To gauge the influence of ambient conditions on loop performance, Saha et al. [10] tested the loop at different temperatures and found less oscillation in temperature profile at higher temperatures due to less heat loss to the surroundings. Also, the MATLAB® and Simulink® models were validated as the transformation of periodic oscillation to chaotic flow due to power rise was on par with the experimental run. The expansion tank connected to the top section can impact the loop stability [11]. As shown in Fig. 1,

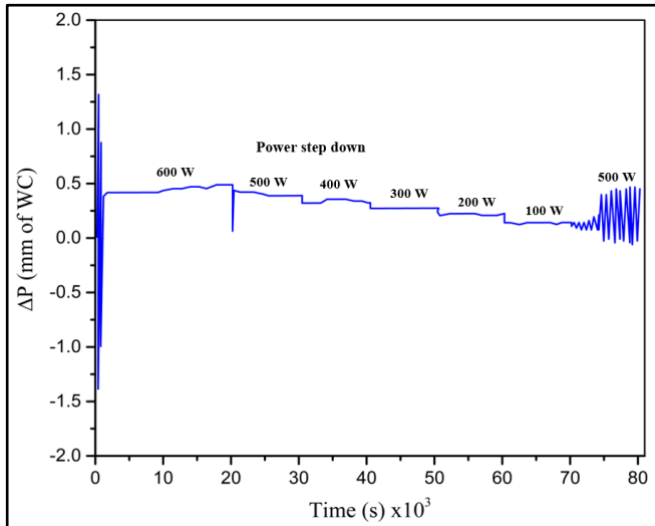


Fig 1: Loop transient behavior during power step down [11]

the analytical model predicted stable behavior in step-down condition until 50 W followed by instability as tank fluid flows to the loop upon contraction. Despite stabilization during step-up, induced instability during step-down suggests the tank connection pipe from the bottom of the loop as discussed in [5]. While the smaller size of the connecting pipe reduces heat loss, a larger diameter is needed for the removal of air pockets. Hence the authors have advised two separate provisions for air removal and fluid expansion.

Generally, the isoflux and isothermal conditions are maintained for heater and cooler respectively. However, intending the waste heat recovery process, Cheng et al. [12] incorporated the end heat exchangers and found the drop-in start-up time as hot fluid entry temperature is raised. The analysis suggested a new correlation (Eq. (4)) over $Nu = 3.66$, as it caused a substantial error. Even the loop geometry was optimized based on the ratio of L_h to L_t to yield maximum steady-state flow rate and heat transfer. In a similar study, Cheng et al. [13] maintained the constant temperature at the cooler and varied both hot and cold fluid flow rate as well as hot fluid temperature. As seen earlier, the start-up time is reduced either with an increase in hot fluid temperature or with the combination of high hot fluid and low cold fluid flow rate. Although the numerical result was consistent with experimental data in terms of stability, more time for stabilization and higher loop temperature were predicted since the analysis didn't consider heat storage.

$$Nu = 0.2702Re^{0.4713} \tag{4}$$

In plenty of studies, the HHHC loop has a symmetric heater. However, an application like electronic cooling necessitates an asymmetric heater. Hence the heater position and loop inclination were varied by Seyyedi et al. [14]. Low cold leg temperature was noticed when the heater was away from it. Further, as reported earlier [15], a smaller loop inclination resulted in stability with a penalty of drop in flow rate (due to deteriorated buoyant force along with increased effective length), which brought the loop to the laminar region from transition and so on. To stabilize the HHHC loop, Arunachala et al. [16] incorporated Tesla valve in the vertical legs and found a unidirectional flow for the entire power range

despite $L_t/d_i < 300$. However, such analysis in a larger diameter loop (instability tendency is high) could further justify its application.

VHVC configuration is known to be the most stable but has the least flow rate as compared to the other configurations. Nie et al. [17] have analyzed such a loop by varying heater power and loop pressure. Although the loop flow rate increased linearly with power at constant pressure, the variation in pressure at constant power did not influence the flow rate. Further, the addition of loop resistance (to stabilize) reduced the flow rate, increasing the temperature difference across the heater. Misale and Frogheri [18] also made such observations, and Elton et al. [19, 20] in the HHHC loop with an orifice.

Although the loop is stable during normal operation in nuclear reactors, instability arises during transients i.e., power rising, power step up, pump trip, feed water failure, and so on. Hence consideration of such transients is of utmost importance. Misale [21] tested the HHHC loop [22] with constant and variable power, which induced instability. The amplitude and frequency of the oscillations and flow reversal tendency were proportional to the power. Following this work, Lokhmanets and Baliga [23] analyzed the loop behavior with power step-up and step-down pattern as such transitional behavior is noticed in the cooling system of the transformer. As the power was increased only upon stabilization, the loop took quite some time to get stable temperatures due to the fluid's thermal inertia and low velocity. NCL application in building heating included VHVC configuration as discussed by Huang et al. [24]. Although the oscillations and loop flow rate increased with power, the larger height difference suppressed the oscillations as the fluid mixing is better along the flow length. Further, the influence of coolant temperature was found to be less significant on loop flow rate.

As real application demands a non-uniform diameter loop, Yun et al. [25] performed a steady-state analysis of a VHVC loop (12.2 m height) to replicate the small modular reactor. The effect of power and loop pressure (5 bar to 150 bar) on flow rate was analyzed (Fig. 2). Although the flow rate

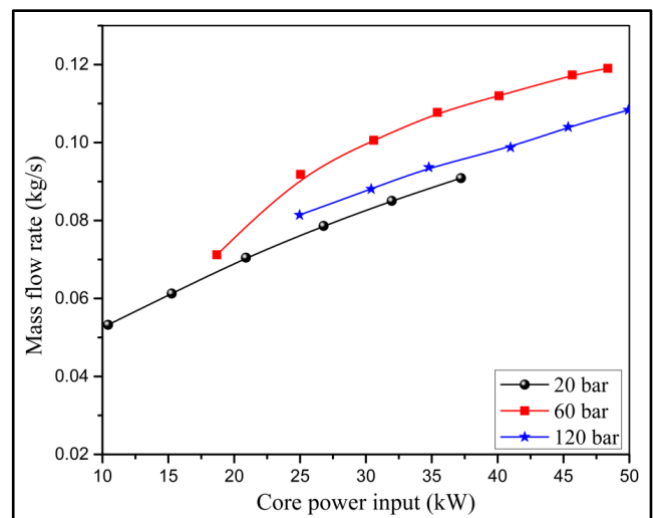


Fig. 2: Variation of flow rate with loop pressure and heater power [25]

increases with power, the unusual behavior of low flow at 150 bar than 60 bar under the same power input was noticed due to thermal property variation of the subcooled water under constant pressure. Even the moving boundary algorithm and lumped component model well predicted the phenomena. Hence, the model was suggested for other orientations and working conditions. A narrow channel finds application in the reactor core, aerospace industry, electronic packaging, etc. In line with it, Zhu et al. [26] have studied the effect of loop inclination (VHHC) and found the highest flow rate in the vertical position of the heater.

NCL in nuclear-powered ships experiences multi kinds of motions, which can cause instability. Wang et al. [27] have compared the rectangular NCL (VHHC) under static and rolling conditions during the pulsating flow and found Nu characteristics in good agreement with Yang et al. [28] when the loop was static. Heat transfer enhancement was noticed during rolling due to induced inertia force (secondary flow) that demolishes the laminarization effect. The rolling of a narrow rectangular loop resulted in less flow rate due to pulsation as observed by Tian et al. [29]. Nu had a close match with yang et al. [28] during the static condition in transition and turbulent regions. However, Sieder – Tate correlation [30] was modified to compromise with the laminar region results. Further, compared to static condition, the heat transfer enhancement was not significant due to the narrow channel. With the experimental setup of [29], Tian et al. [31] have studied the loop having different inclinations. Although the validation of Shah and London correlation [32] for micro and narrow channels is still controversial (Steinke and Kandlikar [33]), the present case had a good agreement of friction factor in the laminar region. However, the predicted friction factor [34, 35] was higher in the turbulent region due to the temperature difference between the heated surface and bulk fluid. The key observations were, drop in flow rate due to reduced effective loop height with an inclination and the presence of additional inertia force during rolling for unsteady state of the loop. A similar study by Yu et al. [36] focused on the loop behavior during the starting stage of the rolling. Due to the influence of fluid inertia, the mass flow change rate lags the angular variation as the relaxation time was low as reported in other studies [27, 29, 31]. Further, the in-house code could well predict the frictional resistance during rolling.

Water in the super-critical phase is also being considered as a coolant in advanced nuclear reactors due to features like system compactness and high thermal performance (density gradient on par with two-phase fluids). In this context, Sharma et al. [37] have done steady-state and stability analysis of the HHHC loop and observed instability for a narrow range of power (7.5 - 8.3 kW) and an operating pressure range of 22.1-22.9 MPa, which was also well predicted by NOLSTA (non-linear stability) code. The high thermal capacity of fluid near the pseudocritical range and subsequent deteriorated interaction with the wall caused such instability. Hence, power rise was suggested when the fluid is close to pseudo-critical temperature.

Zhao et al. [38] suggested NCL for cold collection and storage of radiative cooling, which can substitute the conventional nocturnal radiative cooling system that uses an

electric pump. The system performance was enhanced with a tilt as it increases the effective vertical distance between the heater and cooler. However, the trade-off between the buoyant force and radiation shape factor (between collector and surrounding) decided the optimum tilt as 14°. Hence, for the available cooling flux, the tendency to better water cooling with higher collection efficiency justified its application. Such a system with multiple thermosiphon modules can play an important role in cooling buildings and power plant condensers.

As water is an easily accessible fluid, many researchers have opted for it. However, its low thermal conductivity and density make the HHHC loop unstable and hampers the regular operation. Hence nanofluids have been attempted to eradicate the instability along with better thermal performance as addressed in the next section.

3.2. Nanofluids

Even though NC is preferred for several heat removal applications, the potential threat of flow instability hinders its applications. Although an orifice plate [18-20] in the loop suppresses instability, the subsequent drop in flow rate hampers the heat transfer capability. Hence, several studies have focused on nanoparticles in loop fluid.

The influence of water-based Al₂O₃ nanofluid (0.3 – 2% by weight) on the stability of the HHHC loop was studied by Nayak et al. [39], which yielded a 20-35% higher mass flow rate. The reason being the rise of buoyant force (influence of viscosity is minimal) due to a large change in density (increased temperature difference as specific heat drops) for the same heat input as recorded earlier [40, 41, 42]. In the case of water, due to thermal disturbance in the system, a hot pocket in the loop might have been released from the heater (which was hotter than steady-state temperature), accelerated in the hot leg, and retained even after the cooler section due to less residence time. The opposite phenomenon was true when a cold pocket passed the heater which decelerates the overall flow, leading to a flow reversal. Thus, the oscillations observed are due to the creation of hot and cold pockets. However, due to a higher flow rate of nanofluid, such perturbing forces were suppressed, and stability was attained as shown in Fig. 3. Ho et al. [43] have analyzed a mini HHVC loop with Al₂O₃ nanofluid (0.1 to 1%) and found better heat transfer enhancement as thermal resistance of the loop reduced due to improved convective heat transfer coefficient. However, a decrease in mass flow rate was witnessed for higher nanofluid concentration as viscosity dominates.

The performance of mini HHHC loop with (Al₂O₃ + Deionized water (1 – 3% volume)) was studied under varying input power, loop inclination, and heat sink temperature by Doganay and Turgut [44]. The key observations were the drop in flow velocity with loop inclination (cosine effect) and large nanoparticle size (viscosity effect). The effectiveness was found to be high only in case of low heater power and high heat sink temperature and was proportional to particle size and its concentration, as discussed earlier in case of solar collector [45], plate heat exchanger [46], thermoelectric module [47], and a nanofluid cooled heat sink [48].

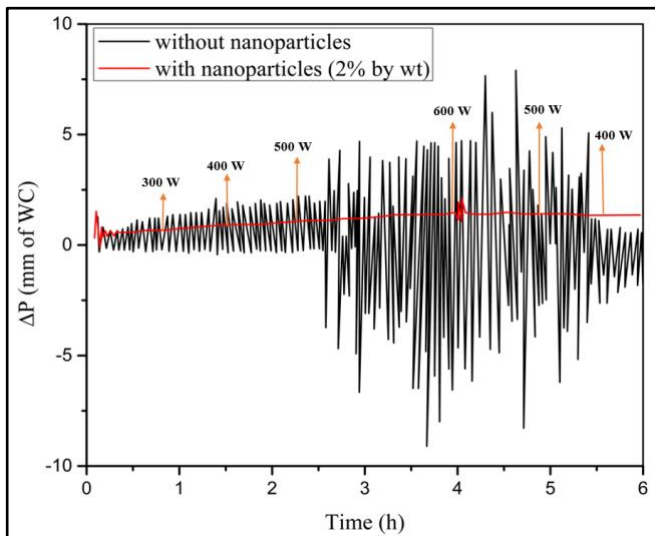


Fig. 3: Suppression of flow instability using nanofluid [39]

Koca et al. [49] have studied the thermal performance with (Ag + water) fluid in a mini loop, intending solar water heating application, and found better performance in vertical position than inclined. Since the heat transfer in the nanofluid loop showed improvement in the numerical study [50] and deterioration in experimental findings [51], the results were put in non-dimensional form i.e., effectiveness parameter (ratio of temperature rise across heater to maximum temperature difference) [44] as heat transfer is not the only deciding parameter. It increased with loop inclination and nanoparticle concentration and decreased with power rise (cooler temperature being constant). Further, in comparison with the Al₂O₃ nanofluid loop [44], the Ag-water combination showed an enhancement in effectiveness with power, while the former had almost constant effectiveness. The stability of Al₂O₃ and CuO fluid based VHVC loop was compared by Shijo et al. [52]. The linear stability analysis [53] showed a stable flow for the entire operating range. While the transient analysis with base fluid shown a delay in the onset of the convection compared to both nanofluids (due to better heat transportation). Although the lower temperature rise across the heater with nanofluids indicated a higher flow rate, the highest enhancement was 12% and 14% respectively due to the trade-off between the particle size and zeta potential. Bejjam et al. [54] compared the behavior of the HHHC loop with various nanofluids (Al₂O₃, CuO, and SiO₂) by varying operating parameters. The results were in good agreement with all previous studies concerning faster steady state, increased mass flow rate, improved Ra, and higher pressure drop compared to water. Amongst different nanofluids, CuO exhibited better performance due to the better thermo-rheological properties.

Hybrid nanofluids were seen to be interesting among researchers lately. Tlili et al. [55] analyzed the HHHC loop with (Al₂O₃+CuO) in water. The stability of the loop improved due to the addition of high thermal conductivity material i.e., Cu in the alumina-based fluid. Although the mass flow rate increased with concentration level until the optimum point, it lay between two base nanofluids (Fig. 4). However, its application is justified as the preparation cost is less. Even the

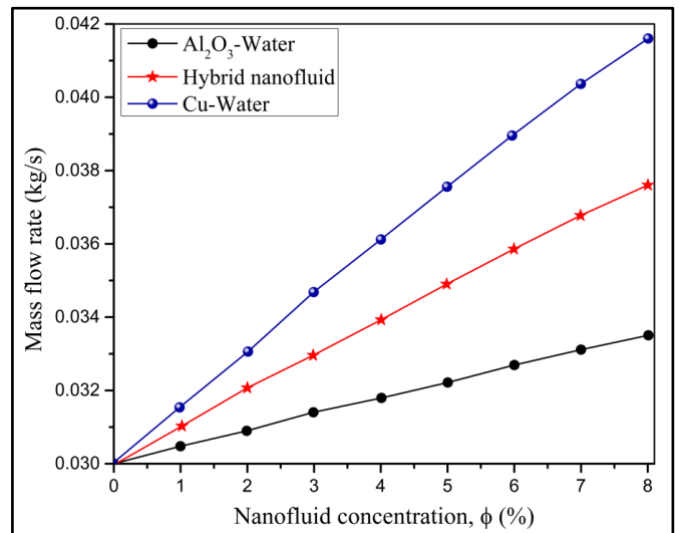


Fig. 4: Mass flow rate variation with nanofluids [55]

phase change nanocapsule material suspensions in water were attempted by Ho et al. [56] in the VHVC mini loop. For the range of heat input, although the drop in hot wall temperature (which indicated better convection) was noticed with the suspension of nanocapsules in the range of 0.1 to 1%, the 0.5% case was optimum due to lower thermal resistance and higher Nu. Hence, at a higher wattage, a high concentration of PCM nanocapsules was suggested.

Although nanofluids enhance the loop performance, the agglomeration and sedimentation effect hinders large-scale application. Hence, CO₂ in super-critical state has been attempted as it exhibits large property variation.

3.3. Super-critical CO₂

Gen IV nuclear reactors found the super-critical NCL as an important inclusion due to simplified design and higher thermal efficiency. Among many fluids, CO₂ is attractive as both temperature and pressure (critical point: 304.14 K and 7.378 MPa) are relatively lower than super-critical water.

As the Boussinesq approximation does not hold good for super-critical fluids, Swapnalee et al. [57] developed a generalized Re correlation (Eq. 5) for water and CO₂ in a super-critical state considering dimensionless density and enthalpy, which was also in good agreement with other super-critical fluids mentioned in the literature.

$$Re = C \left[\frac{Gr_m^*}{N_G} \right]^{0.364} \quad (5)$$

Where, C = constant based on dimensionless density and enthalpy.

The steady-state analysis of the VHHC loop reported the minimal influence of loop pressure on flow rate compared to the coolant entry temperature [58]. Further, the variation of flow rate with power is shown in Fig. 5. Since both frictional resistance and buoyancy force are the function of density and as density difference depends on heater and fluid pseudo-critical temperature, mass flow rate increases up to a particular level (buoyancy dominant region) and reduces later (friction

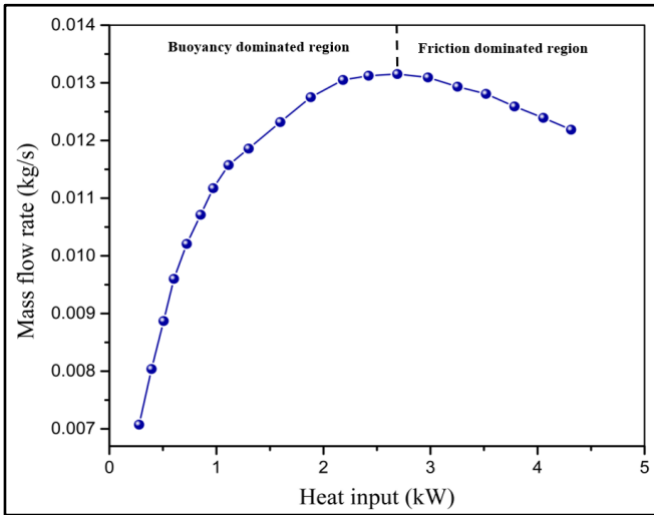


Fig. 5: Mass flow rate variation with power [58]

dominant region). However, no sign of instability was observed as the outlet temperature of the heater was in the pseudocritical region.

In the VHHC loop, Liu et al. [59] observed the maximum heat transfer coefficient as bulk enthalpy increases due to a sharp rise of specific heat in the pseudo-critical region. At this point, even though the bulk fluid temperature is slightly lower than the pseudo-critical state, the fluid temperature in the vicinity of the wall has already attained a critical state. On the other hand, an increase in heat flux resulted in heat transfer deterioration due to the temperature of bulk fluid being < pseudo critical < high wall temperature. This is the barrier for sCO₂ application in the nuclear reactor, which could be avoided on proper design. Further, the Nu correlation developed (Eq. 6) has a mean error of 2.2% compared to others [60-63] being in the range of 30% to 60%.

$$Nu = 0.0022Re_b^{1.03}\overline{Pr}_b^{0.58}\left(\frac{\rho_w}{\rho_b}\right)^{0.57}Bu^{0.026} \quad (6)$$

In continuation, Liu et al. [64] observed instability when the HTF temperature at the heater exit was more than the pseudo critical temperature in the loop [58, 59]. Due to a significant change in density near the pseudo-critical point, the thermal expansion in the axial and radial direction led to noticeable buoyancy and flow acceleration effect, in which the former is more dominant [59, 65] in the heat transfer analysis. When the bulk flow temperature is less than the pseudo-critical point, it reduces velocity gradient and shear stress. Further, the generation and diffusion of turbulence in this region get restrained, deteriorating heat transfer from the wall to bulk fluid. With further density difference, fluid near the wall gets accelerated which restores the generation and diffusion of turbulence thus changing the heat transfer mode from deteriorated to normal. As turbulence was restored, radial fluctuation of fluid particles near the wall became noticeable. Due to it, low-temperature fluid particle (A0) in bulk flow can interact with the hot wall and expands (A1). Later it contracts as it mixes with the bulk flow (A2). Such expansion and contraction led to pressure variation in the loop (Fig. 6). However, system stability is possible with higher loop pressure and local resistance. Recently, Lie et al. [66] have

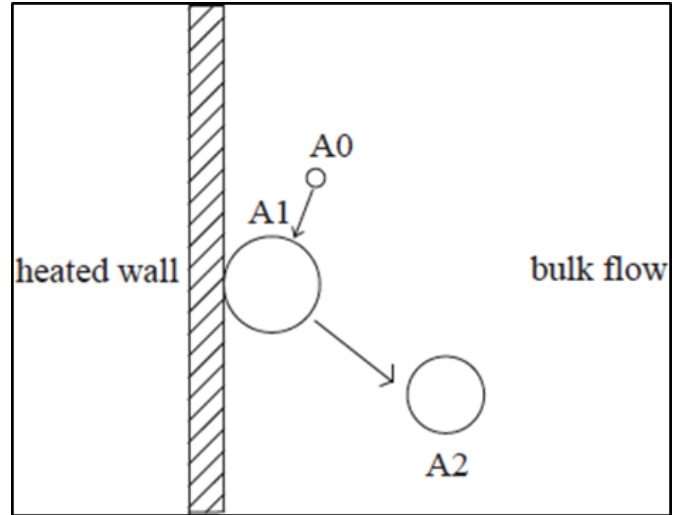


Fig. 6: Expansion and contraction of the fluid particle [64]

developed, validated, and compared a 1D analytical model [36,67,68], which is similar to Vijayan's model [4] (Eq. 7). The study highlighted that NC enhancement is possible by keeping the inlet temperature of HTF in the loop lower than the pseudocritical temperature.

$$w_{ss} = \left(\frac{2b\rho_{pc}^2\beta_{pc}gA^2Q\Delta z}{RC_{p,pc}}\right)^{\frac{1}{3}} \quad (7)$$

The near-critical CO₂ (from subcritical to super-critical state) state was discussed by Chen et al. [69] using a mini HHHC loop. Although instability occurred with charge pressure being less than the critical point, a transition from unstable to stable condition was evident at a pressure of 7.38 MPa. Even greater influence of cooler temperature on stability was observed. Zhang et al. [70] have observed the flow instability when the outlet temperature at the heater was way beyond the pseudocritical temperature. Even numerical codes viz., Special Predictions of Reactor Transients and Stability (SPORTS), and Canadian algorithm for thermal-hydraulic network analysis (CATHENA) gave satisfactory results.

Air as a coolant in NCL finds application like electronic cooling, space heating, etc. In a study by Sadhu et al. [71], a reduction in air velocity led to a rise in the loop temperature, pressure and drop-in flow rate. Further, to simulate accidental failures, the fan was switched OFF, which resulted in a steep rise of loop pressure for high charge and temperature rise for the low charge of fluid. Hence charge level emerged as an important factor during the design. The data were carried forward to develop Re correlation (Eq. 8), which deviated from Vijayan [6], Chen et al. [72], and Yadav et al. [73] as the geometric parameters and fluid were different. The transient

$$Re_{ss} = 1.368\left(\frac{Gr_m}{N_G}\right)^{0.452} \quad (8)$$

behaviour during the start-up/shutdown/power step was undertaken by Sadhu et al. [74] in continuation of their previous work [71]. During start-up and shutdown, the variation of loop temperature and pressure was sudden in the beginning and followed by gradual change. However, during the fan failure analysis, a sudden rise in temperature and

pressure was observed, which could be catastrophic. Hence such observations need to be addressed during system design as they directly imitated load rise, load reduction, shut down, and coolant loss scenarios.

Transitional behavior and effect of operating parameters in HHC loop were studied by Deng et al. [75]. The validated numerical model could predict stable, unidirectional and chaotic pulsing flow patterns fairly well. The influence of cooling rather than heat input was significant for the loop behavior. Further, upon reducing the cooling condition to the critical temperature, the loop became unstable and couldn't stabilize even when the heater power was reduced as the fluid property was too different.

Yadav et al. [76] have studied the loop inclination effect in the sub and super-critical region using end heat exchangers, which resulted in same time for the steady state with tilt in XY and YZ. plane (Fig. 7). However, the tilt in YZ. plane caused a rise in loop temperature (reduced effective height - lower buoyancy effect) against reduced the loop temperature with XY plane due to initiation of unidirectional flow. Unlike the constant heat flux source [77], this setting couldn't exhibit pulsating flow. With earlier configuration [76], steady-state behavior in subcritical and super-critical phases was studied by Thippeswamy and Yadav [78]. The heat transfer enhancement seen was 800% and 400% respectively in the super-critical and subcritical state compared to water as loop fluid. For low-temperature applications (below 0 °C), subcritical liquid CO₂ yielded a maximum 500% higher heat transfer rate compared to the brine solution.

The limitation with sCO₂ is the fluid should be near the pseudocritical region to show high NC ability, which is very difficult during accidental scenarios in NPP or other applications. Hence, liquids having very good thermal properties at atmospheric conditions are always favorable.

3.4. Liquid metals

Some of the GEN IV reactors use liquid metal as a coolant due to better thermohydraulic properties at atmospheric pressure over conventional coolants. The high boiling point of liquid metals makes it an ideal coolant in nuclear reactors which could avoid the issue of polonium.

In VHHC configuration, Naphade et al. [79] used Lead Bismuth Eutectic (LBE) to study the steady-state characteristi

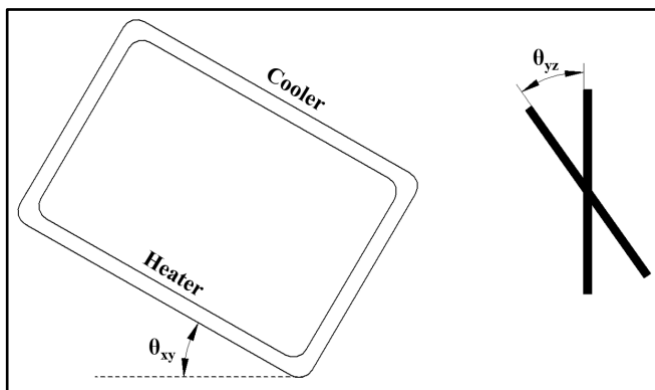


Fig. 7: Inclination angle for loop in both axes [76]

cs and to validate the CFD model. The time taken for steady state was very low due to the favorable thermo-physical properties of the fluid. Further, the heat loss in the experiments resulted in a lower mass flow rate compared to CFD. Borgohain et al. [80] used air as a coolant for powers up to 2400 W and water for up to 5000 W to analyze steady-state and transient analysis in the VHHC loop. Considerable deviation with Vijayan correlation [6] was seen at low powers as axial heat conduction not being incorporated in the model as well as due to considerable heat loss at higher power. All transient studies viz., start up, loss of heat sink, power step, and coolant flow rate change, showed a rapid variation in heater outlet temperature, which could reduce the life of the material due to thermal cycling. Further, the Lead Bismuth Eutectic Natural Circulation (LeBENC), an in-house 1D code had a good agreement at lower power but deviated at higher power due to the effect of expansion tank interaction with the loop fluid. Hence, a multi-dimensional feature in the code was suggested to predict such a phenomenon accurately. Focusing the VHVC configuration, Shin et al. [81] studied steady-state performance in the test loop i.e. HELIOS (heavy eutectic liquid metal loop for integral test of operability and safety of PEACER (proliferation-resistant, environment-friendly, accident-tolerant, continual and economical reactor)) by maintaining the perfect adiabatic wall boundary condition with local loop heaters and validated the MARS-LBE (Multi-dimensional analysis of reactor safety using LBE) code. A complete stable flow was witnessed for power up to 33.6 kW. The mass flow rate and the temperature difference between hot and cold legs were predicted with less than 7% error, but the absolute temperature distribution within the loop was underestimated by as much as 25 °C due to the wrong selection of heat transfer correlation. This discrepancy could not be confirmed as the heat transfer measurement on the cooler side was not adequate.

Ryu et al. [82] performed the instability analysis of LBE loop during the initial heat up in a reactor with a KIMM LIMSI (Korea Institute of Machinery and Materials – Liquid metal simulation) system. The NC was seen to develop within 500 s due to the high thermal expansion coefficient. An introduction of the bubble injection system was the highlight of the study. During transient analyses like loss of coolant accident (LOCA) and transient overpower (TOP), the loop flow rate needs to be accelerated to avoid instability in the system. As depicted in Fig. 8, the flow rate was increased by 125 to 275 % when the bubbles were injected at the top section compared to 75 to 100% rise when injected at the middle of the riser. As the density of air is less than the liquid metal, the flow was directed upwards which reduced the resistance of flow along the line.

NPP prefers liquid metals as NC flow is quick and stable due to high thermal expansion coefficient and density. However, the heat transport capacity is less than water [1]. Hence molten salt is justified as explained in the next section.

3.5. Molten salts

Low melting and high boiling point of molten salt attracted the reactor core cooling as well as solar thermal applications. With a VHHC arrangement, Srivastava et al. [83]

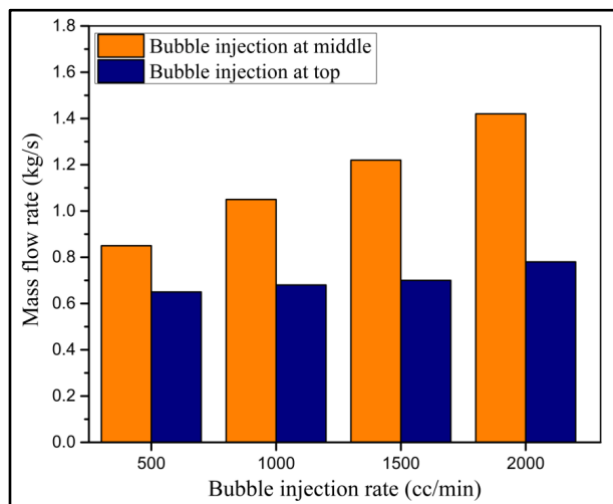


Fig. 8: Effect of bubble injection [82]

performed steady state and transient experiments using a mixture of NaNO_3 (60%) and KNO_3 (40%) salt. An overprediction by Vijayan correlation [6] was due to the uncontrolled heat loss in the loop despite the adequate insulation. However, the LeBENC code also overpredicted the result (even though the heat loss was accounted for) due to the unchanged heat loss coefficient value. In the transient studies viz., loss of heat sink and power step change agreed well with the code. In a similar loop [83], the steady state and transient results have been compared with CFD by Kudariyawar et al. [84], which showed a good agreement. The reason for achieving such a good agreement was due to the modeling of the expansion tank in the CFD study. The ideal range of power preferred was such that the loop fluid should lie between the freezing point ($238\text{ }^\circ\text{C}$) and the salt composition zone ($600\text{ }^\circ\text{C}$).

The construction, maintenance, and experimental analysis of molten salt loops require a lot of investments. Hence scaled-down system can be the solution. Shin et al. [85] adopted a similar procedure to scale down a fluoride based high temperature molten salt reactor (FHR and KALIMER) and used DOWTHERM RP as the simulant liquid based on matching of the Pr value. The attempt to validate with Vijayan correlation [6] and Scarlat correlation [86] resulted in decent agreement. Even the MARS code and ANSYS CFX were validated with the present experimental work, which confirmed the benefit of scaling analysis. Further, an experimental analysis of FLiBe molten salt based loop by Britsch et al. [87] highlighted the benefits of fluid, operational difficulties, flow phenomenon and the effect of salt degradation. Simulation of such experimental work was quoted as future scope.

Since molten salts are very difficult to maintain as they undergo solidification and cause corrosion of the container, researchers have used materials like Inconel 625 [83, 84]. Hence, few other fluids have also been experimented based on the kind of application and operating conditions.

3.6. Other fluids

Some researchers have worked on fluids that have a low

operating range, which finds application in electronic packaging. Cataldo and Thome [88] have varied the charge of R1234ze, R1234yf, and R134a for cooling a transistor module, with a specific focus on the overall thermal resistance and flow rate. Since the fluid with high charge exhibited critical flux condition, a low charge was suggested. However, the low charge of R1234ze induced instability, which wasn't noticed at a high charge. At this condition, it had a lower flow rate compared to R1234yf, which had fulfilled all the requirements of the heat load in a transistor for a low charge. A similar thermal performance was also seen in R134a, but due to its high global warming potential (GWP) value, R1234yf was finally suggested.

To improve the performance of conventional single slope solar still, the air was the NC fluid as studied by Rahamani et al. [89]. The airflow (due to density variation) would rise in the solar still with the vapor towards the condenser, which returned to the solar still after condensation and the cycle continued. The conventional solar stills do not have the condenser separately. Hence the modified geometry increased the temperature difference between the still and condenser. The analytical model developed based on the experimental data showed a good agreement with Vijayan's model [6], whereas Dunkle's model underpredicted the results. Since Dunkle's model is used for cavities with evaporative surfaces and parallel condensing, whereas in the solar still air convection created by the NC led to the improvement in heat transfer, a higher value was predicted.

Not much work has been dedicated towards NC in low temperature application and can be thought off by using different fluids and design configurations as the behavior of loops in such a low operating range is still not clear and a difficult task for experimental accuracy.

4. Coupled natural circulation loops

Although the CNCL is applicable in solar thermal power plants, decay heat removal, and diverse passive fuel cooling system in nuclear reactors, the extent of research is limited compared to NCL. Hence this section comprehensively addresses all studies to date, which are subclassified as general studies, application in nuclear power plants, and solar thermal systems.

4.1 General studies

One of the oldest articles on CNCL is by Zvirin et al. [90], which dealt with the experimental and theoretical study. The set up included two parallel loops with a heater and two heat exchangers. Out of two heater designs tested, the spiral type gave a better rise in temperature due to uniform heating in the core compared to the immersion type. Further, a reasonable agreement was observed between experimental and theoretical results. An analytical study by David and Roppo [91] discussed the flow behavior in a thermally coupled loop. When the heating is identical in two loops, the model gave stable counter-current flow for the range near to critical Ra. Later, flow reversal and change of flow direction led to chaotic behavior. A numerical (1D) study by Salazar et al. [92] considered two arbitrary shaped loops coupled together with

only heat being exchanged. Due to flow behavior dependence on heat flux, the authors had suggested the consideration of more general boundary conditions in addition to the multi-dimensional motion mechanism for better prediction.

Ehrhard et al. [93] were one of the pioneers to work on experimental toroidal coupled loops and found the possibility of steady co-current flow by giving small power steps. However, with larger power steps, flow is established with different flow directions in the two loops. Satoh et al. [94] have numerically analyzed the instability in double toroidal loops where the bottom tube is given constant heat flux and top tubes are cooled. A validated 1D CFD model was used for studying the non-linear effects of the flow. Both symmetric and asymmetric initial conditions were imposed and found a double loop system as complex due to the existence of five flow regimes against three in a single loop system. The flow characteristics and effect of connecting the tube in a θ - loop were investigated by Satou et al. [95], which had the top portion at constant temperature and the bottom half at constant heat flux. The key observation was loop tends to suppress the chaotic behavior with inclination.

Marchitto and Misale [96] have investigated the flow and heat transfer phenomenon in parallel loops whose heater ends are interconnected (Fig. 9). Multiple tests were conducted to understand the mutual influence of connected loops, including equal heating with and without interconnection, and differential heating. It was seen that the highest ΔT average (amongst legs) was for the loops without interconnection and least for differentially heated loops with interconnection (due to the fresh liquid in the connecting tubes of the two loops that participate). Further, all the experimental results were compared with Vijayan [6] correlations and found good agreement. The vertical and horizontal coupled natural circulation loops were analyzed using 1D analytical model and later verified with the 3D CFD model by Dass and Gedupudi [97]. Authors have suggested a 1D model due to less computa-

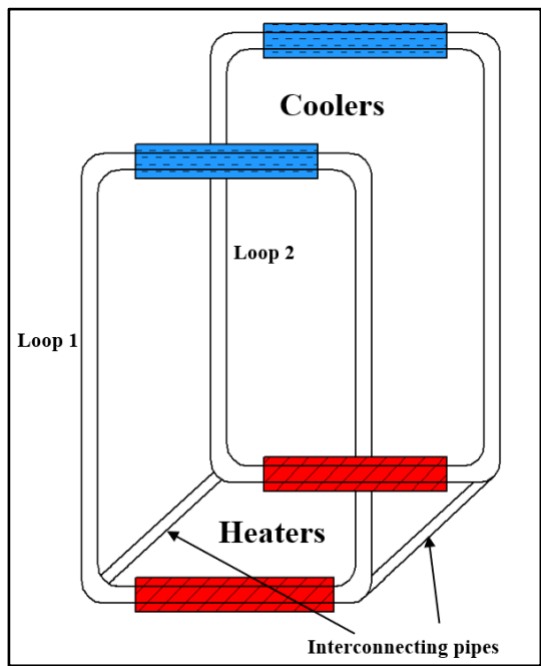


Fig. 9: Parallel loops with interconnection [96]

tional time, robustness, absence of geometry creation, mesh generation time, and better accuracy. Further, the studies on the influence of heater-cooler arrangement showed vertical CNCL always exhibits counterflow arrangement for all the heater-cooler configurations. However, horizontal CNCL shuffles between parallel flow and counter flow based on heater-cooler configurations.

4.2 Application in nuclear power plants

CNCL applications in nuclear plants include power plant cycle, decay heat removal system, and moderator cooling system.

Cheng et al. [98] have performed transient analysis (RELAP-3D) to gauge the efficacy of the decay heat removal system of the proposed GEN IV gas-cooled fast reactor, which had a combination of active and passive systems. During station blackout, hot helium was recirculated from the emergency cooling system (ECS) between the reactor and the Heatric heat exchanger through a battery-powered blower. The other end of the heat exchanger was connected to the dump heat exchanger by a water line (natural circulation). Finally, the dump heat exchanger loop was cooled externally with circulating water from the spray pool (Fig. 10). The helium line was powered to remove the high-intensity heat generated in the core. Later, when the core heat generated was reduced to 2%, the blower was switched OFF and the natural circulation in the helium loop begins. Thus, the transient analysis of such CNCL revealed its feasibility and can be incorporated in NPP. In continuation, Cheng et al. [99] have also addressed the concept of autonomous systems for decay heat removal. It was proposed to run parallel during normal operation with the primary power conversion units, thus increasing plant efficiency. Although it replicated the previous ECS system, the concept was treated as semi-passive due to the presence of turbomachinery. Here the NC can be effective if loop fluid density is elevated (pressurization).

Many analytical/numerical analyses justified the concept of passive decay heat removal system coupled with modern nuclear reactors. However, to ensure its capability, Krepper

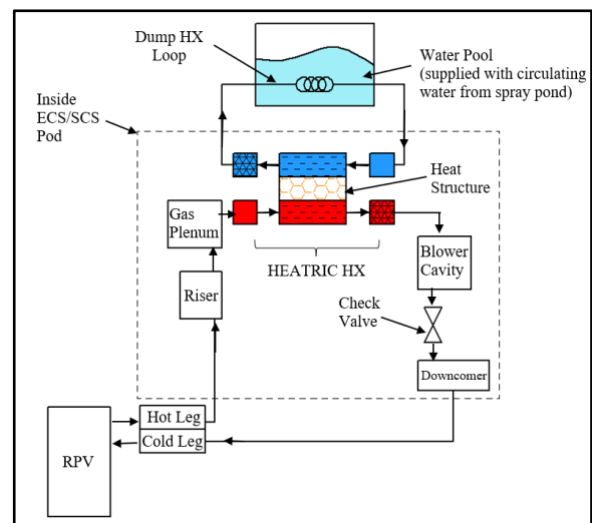


Fig. 10: Schematic of an emergency cooling loop [98]

and Beyer [100] have validated the CFD model for an Economic simplified boiling water reactor (ESBWR) emergency condenser. Figure 11 shows a reactor with an upper plenum where the steam line connected to the emergency condenser and the outlet being the bottom of the reactor. During normal operation (left side in Fig. 11), there is no steam generated and during station blackout, the water level in the core reduces (right side in Fig. 11), forming steam that condenses back to water (in geodetic flooding pool) and returns to the bottom of the reactor pressure vessel. Further, the thermal stratification study was also conducted to check the reliability of experimental results as well as to validate the CFD code.

A complete NC loop of a Lead cooled fast breeder reactor (LFBR) was analyzed by Damiani et al. [101] to understand the behavior during decay heat removal. The complete process was happened due to the formulation of hot and cold legs. Such simulation revealed very good decay heat removal (initial 2 hours) keeping the lead operating range safe without operator interference. In continuation, Damiani et al. [102] have suggested an isolation condenser in place of the air-cooled condenser [101] since it had better heat transportation capability. Figure 12 shows an emergency cooldown tank (as

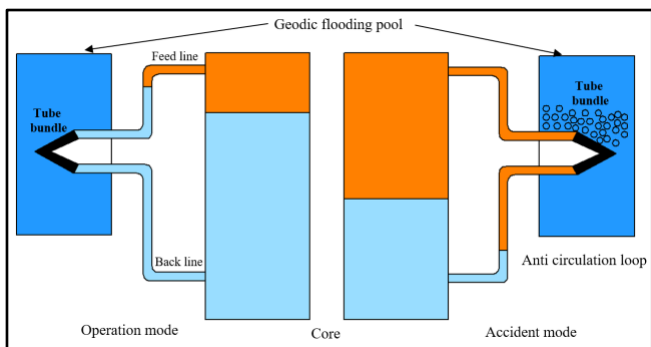


Fig. 11: Operation scheme of an emergency condenser [100]

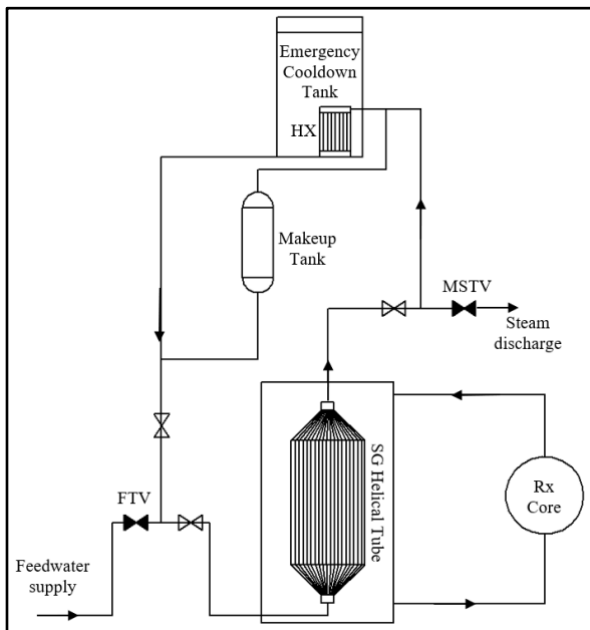


Fig. 12: Schematic of SMART passive residual heat removal system [103]

an ultimate heat sink) that works to cool the reactor core via the steam generator [103]. The primary loop was between the reactor and steam generator, which in turn had a series loop connecting the emergency cooldown tank. The effect of the radial position of the tube and tube bundle on heat transfer was the main objective of the study. This experimental analysis demonstrated the SMART (System-integrated Modular Advanced Reactor) design, which showed a high confidence level to take action before core damage could occur.

Ono et al. [104] have performed experiments applicable to Japan Sodium - cooled Fast Reactor (JSFR) as shown in Fig. 13. The Ri (Richardson number) similarity was considered in the analysis with a scale ranging from 1/6th to 1/8th. The direct reactor auxiliary cooling system (DRACS) was under NC which had a dipped heat exchanger (DHX) and an air conditioner to replicate the end use. Both the primary reactor auxiliary cooling system (PRACS) and DRACS come under the decay heat removal system. In the transient study, the pump shut down in both primary and secondary loops affects the flow rate of the fluid. The NC in primary loop initiates as the air damper opens and hence a gradual increase in air velocity is noticed. A delay in NC was noticed as there is a time gap for the heat transfer to the sodium. A transient study (using RELAP5/MOD 3.4) by Lv et al. [105] targeted a passive residual heat removal system of a PWR reactor that had a parallel-series NCLs. During an emergency, the steam generated is directed towards the cooling water tank and the condensate flows back to the steam generator. The inventory in the tank is sufficient during sudden station blackout and later secondary loop activates (due to the rise of water temperature) which finally dumps heat into the atmosphere via an air heat exchanger.

Apart from nuclear reactor cooling, moderator cooling is also important during extended station blackout conditions. Hence Pal et al. [106] have studied the scaled-down model of the passive moderator cooling system applicable to Advanced heavy water reactor (AHWR). This series-coupled loop includes Calandria (as a heat source), water pool (as a heat sink), and heat exchanger as an intermediate element. The power step up/step down experiments were performed to study the loop behavior. Even CFD analysis was done for the primary loop, which showed close agreement at lower power only as heat loss was considerable at high powers. Similarly,

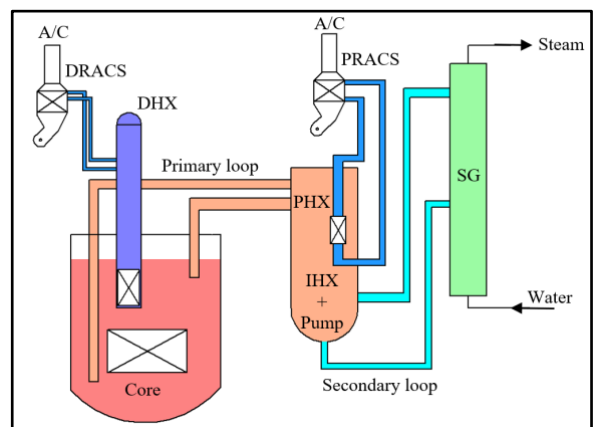


Fig. 13: Heat transport system of JSFR [104]

Kumar et al. [107] have conducted experiments, analyzed using system code RELAP5/MOD 3.2, and performed CFD simulations to know the temperature distribution within the Calandria. Both primary and secondary loops are initially stagnant as only local convection currents were generated in Calandria, which was observed in experiments and CFD. However, RELAP couldn't trace this mechanism due to limitations with the code. Nevertheless, the initialization of the primary loop followed by the secondary loop was properly captured by the code.

An integral scaled test loop facility for AHWR was used to analyze the coupled behavior of the main heat transport system, isolation condenser and pool by Kumar et al. [108] as shown in Fig. 14. During station blackout simulation, the steam outlet is diverted to the isolation condenser (in water pool) and condensate returns to the reactor through the steam drum. The performance of the isolation condenser gauges the ability of decay heat removal. In the beginning, the temperature gradient is zero, later rises, and becomes stable before the inception of boiling. Once the boiling starts, stratification breaks due to faster mixing, and hence temperature gradient falls. Hence, it was concluded that the design of the isolation condenser is important to ensure heat removal during all the zones. Even RELAP5/MOD 3.2 analyzed the thermal stratification well for the pool with a volume pool model than one volume model.

A generic concept of a diverse low-pressure passive fuel cooling system was proposed by Vijayan et al. [109] that could be applied to any nuclear reactor. The chance of LOCA in high- pressure water-cooling systems (present loops) is eliminated as low- pressure system is introduced. As shown in the schematic (Fig. 15), the LBE loop absorbed the heat from the lead and cooled by atmospheric air from the 3rd loop. A thermoelectric generator was also proposed to be installed in

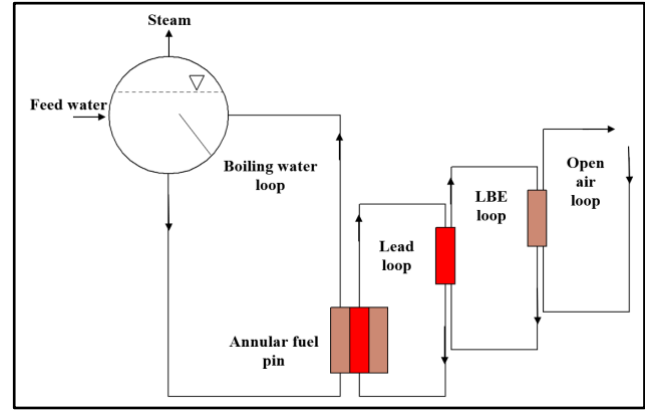


Fig. 15: Coupled series loop [109]

between the air heat exchanger for backup power generation. To check the feasibility of the system, steady state analysis was done with a maximum of 6% full power and noticed that the air temperature is 335 °C, which is practically possible. During the analysis, the decay power was taken as the base point for conservative analysis. Hence, authors have concluded that situations like Fukushima can be avoided with the proposed system that could also generate power up to 20 days from the thermoelectric generators besides the infinite passive cooling directly done from the fuel rods.

4.3 Solar thermal applications

Although to date CNCL based research is mainly focused on decay heat removal systems due to their criticality, very few articles have proposed the configuration in a solar thermal power plant.

With the beam down concept being implemented in solar thermal power plants, the heat source is made available at ground level which opens the opportunity for implementing NCL. In this context, Vijayan et al. [110] proposed the coupled series loop as shown in Fig. 16. Molten salt recirculates within the integral receiver (concentrated solar flux), molten salt recirculates, and at the other end, the atmosphere is heat sink as air-cooled condenser is adopted. Further, Thalange et al. [111] have proposed the new configuration of CNCL through 3D CFD simulations. As shown in Fig. 17, the system consists of a heat exchange tank (HX6), a hemispherical receiver, and an interconnecting pipe to form a closed molten salt loop. Within the HX6, riser (8A)

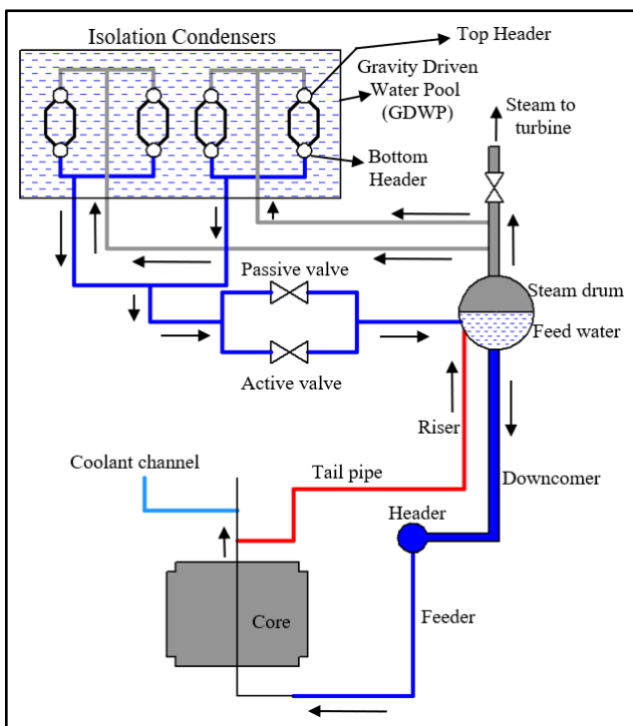


Fig. 14: Schematic of cooling system in AHWR [108]

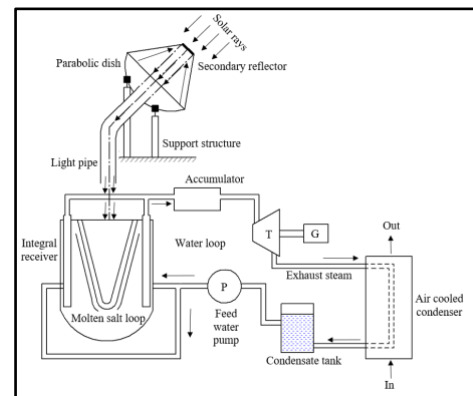


Fig. 16: Schematic of the mini solar plant [110]

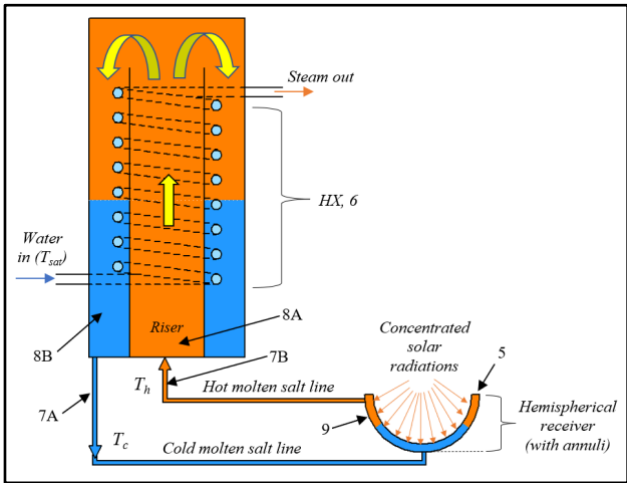


Fig. 17: CNCL for solar thermal power plant [111]

and downcomer (8B) is situated. The spiral HX in the downcomer and power system forms the water-steam loop. The optimized design could extract 300 kW of heat by maintaining a convective coefficient of 103 W/m²K and 42 W/m²K at heater (receiver) and cooler (steam generator) respectively.

5. Preliminary study

CNCL studies are mostly analytical and/or numerical against a very few experimental studies, which has water as the final sink for decay heat removal. However, the system can be more reliable if the atmosphere is treated as the heat sink [109]. Hence the present preliminary study addresses the steady state analysis of the HHHC coupled series loop where the atmosphere acts as an infinite inventory for cooling.

5.1 Experimental set up

It includes three NCLs in series (two closed loops and one open loop). The Lt/D ratio for the first and second loop is 139 and 325 respectively, with a total height of more than 8m. The 1st loop heater is an electrical resistance type, and the double pipe heat exchanger is the cooler [110]. The heater of the 2nd loop would be the cooler of the 1st loop. The cooler of the 2nd loop is a finned tube to which the open loop is connected as shown in Fig. 18(a). In the 3D numerical study by Elton et al. [112], a copper finned tube was designed and optimized. Here, offset fins were opted for better heat transfer.

All the loops are properly insulated with ceramic wool and PVC pipe. K-type (mineral insulated, 1.5 mm diameter (nut and ferrule - stem type)) thermocouples are used at multiple locations as shown in Fig. 18(b). In 1st loop, across the heater and cooler, sixteen thermocouples (four at every junction) are attached (T1-T16). To measure the average temperature of the heater, three more probes are used (T17-T19). The difference between insulated outer surface (T20) and ambient (T21) temperature decides the quality of insulation. In the 2nd loop, across both heater and cooler, eight thermocouples (two each at every junction) are attached (T22-T29). The difference between ambient (T30) and insulated outer surface (T31, T37) temperature decides the quality of insulation in the 2nd loop. Air entry (T32, T33) and exit (T34, T35) temperatures are

recorded in an open loop. T36 and T38 measure the insulated outer surface of open loop. Lastly, T39 and T40 show the free end and base temperature of the fin.

The differential pressure transmitter (Rosemount and Honeywell) measures pressure drop (to calculate mass flow rate) across the 1st and 2nd loop heater section. Dimmer stat (Auto electric) and power analyzer (Yokogawa) combination is used to supply a known amount of power to the 1st loop. A hot wire anemometer (Testo) is used at the exit of the open loop to record the velocity and temperature. The output from thermocouples, pressure transmitter, and power analyzer are recorded by a data logger (Keysight).

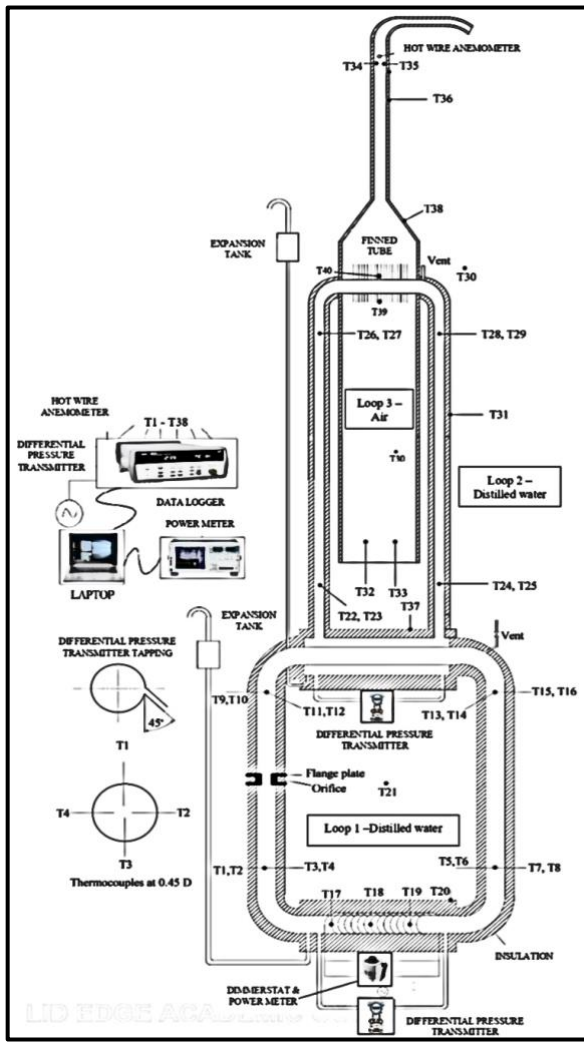
Initially, both the loops are filled with distilled water and the entrapped air bubbles are removed through the vent. Once all the instruments are set, the known heater power is given to the 1st loop and simultaneously all the parameters are recorded with a scan time of 5 s. For the given heater power, the loop may take 18 to 24 h to attain steady state. The experiments were conducted until the stability threshold is obtained for the 1st loop, which is less than the earlier case [5] due to reduced heat extraction at the sink side.

5.2 Results and discussion

The power was varied from 20 W to 45 W after which the loop showed instability. A bar graph (Fig. 19) highlighting the



(a) Photograph



(b) Schematic
Fig. 18: CNCL set up

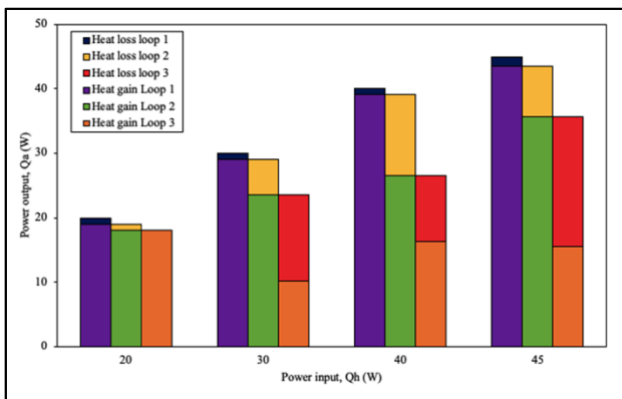


Fig. 19: Heat flow pattern

amount of heat transferred from 1st loop to 3rd loop along with the individual heat loss. The heat loss in all the loops started rising with an increase in power. Since the specific heat of air is low (1/4th of water), it didn't carry substantial heat from the finned tube as efficiently as water transports heat in the 1st and 2nd loop. Hence for higher powers, the bulk mean temperature of the system increased. The net heat transferred from 1st loop to 2nd loop is in the range of 85 to 100%, from 2nd loop to 3rd

loop in the range of 40 to 80%, and from 3rd loop to ambient at 45 to 100%. It can be noticed that the ambient temperature plays a very important role in the air velocity and heat loss of the system, as it gets really hot in the noon compared to the cold wind in the nights.

The mass flow rates recorded in the 1st, 2nd and 3rd loop are plotted against power as seen in Fig. 20. It can be seen that there is a non-linear increase in the mass flow rate. This could be due to the dominance of frictional resistance at higher powers. The mass flow rate for the 2nd loop is seen to be low compared to 1st due to lower diameter (more frictional resistance) and reduced heat transfer from 1st loop to it. Even the increasing trend is not significant as compared to the 1st loop. Further, the mass flow rate in the open loop has seen a nominal increment. Higher hydraulic resistance and less driving force (low ΔT between finned tube surface and air) are the reason for it. The trend of reduced flow rate in each loop is also complemented by the temperature difference across the heater (Fig. 21). Although the temperature difference (ΔT) increases with power, the highest value is observed in the open loop, followed by the 2nd loop and the least being in the 1st loop.

Since the concept of series coupling works, a modified version of it can be implemented for decay heat removal. In the present study, the experiments were not conducted at higher heat input due to the limitation of loop fluid boiling point. However, the heat transfer fluid having a higher boiling point will suffice the purpose as driving force increase in open loop upon the rise in finned tube surface temperature [109].

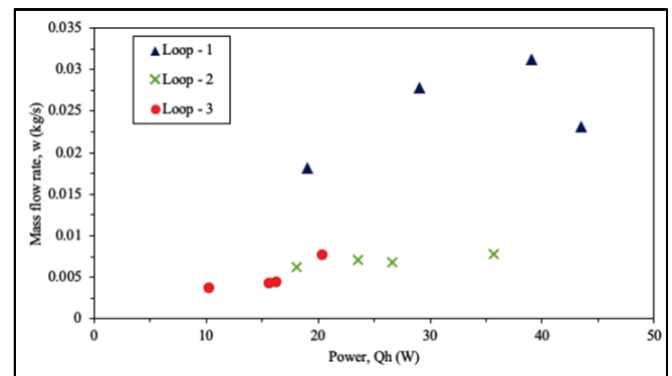


Fig. 20: Individual loop mass flow rate vs power

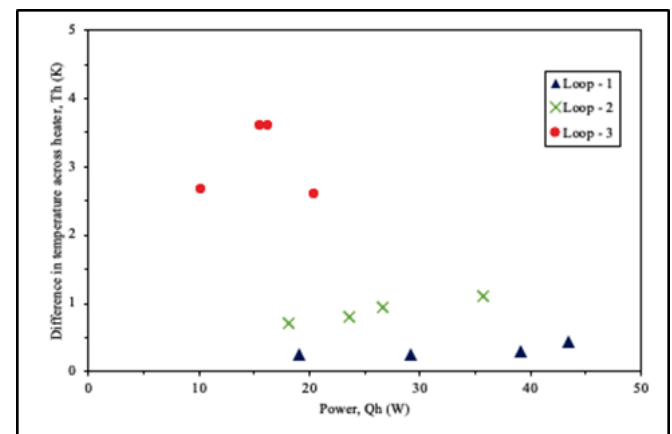


Fig. 21: Temperature difference across heater

6. Conclusion and future scope

Plenty of research is being carried out in SPNCL due to easy maintenance, reliability, and adoption of low to medium power operating range (majority of the engineering applications lie in this category). The user end application binds the heater and cooler's orientation and operational and geometrical parameters. Most of the studies have presented the experimental methodology and/or validated numerical algorithms mentioning instability regimes considering water as the heat transfer fluid. The salient observations were the higher mass flow rate in the larger diameter loop compared to the lower diameter at the cost of a lower stability threshold value. Even the flow rate enhancement with the height of the loop as well as nanofluid was highlighted. Apart from other heat transfer fluids, $s\text{CO}_2$ is finding application in NCL with improved performance as compared to other single-phase fluids, but such systems should be very sturdy to withstand high pressure.

Concerning the stability of the system, fluids play a major role followed by other geometrical parameters. The specific heat capacity of the fluid is an important parameter that reduces the size of the hot plug formed thus increasing the stability threshold of the system. It was noticed that even though FC43 has a higher density than water, the loop remained unstable due to low heat capacity [18]. The most economical way of stabilizing an NCL is the addition of an orifice plate or other devices to increase the local resistance as the cost of nanoparticles or altering the geometry of the loop would be difficult. Few researchers were also thought of loop inclination and bubble injection. Further, stability gains importance in marine systems as the loop is experiencing complex motion. From the heat removal point of view in the reactors (which is mostly the accidental scenarios), the NCL would efficiently cool the system while in stable or unstable regime. However, instability matters the quality of power generation.

In most of the experimental works, no clarity is given about instrumentation and data interpretation. For example, when the loop diameter is large, the pressure drop recorded is of the order of 1 Pa, which is quite low to measure for any pressure transmitter. The use of an inline flow meter in such a situation can add resistance to the loop, thereby changing the stability regime. As the loop diameter increases, 3D flow is quite possible, which demands multiple sensors (4-5) for temperature measurement at a section.

Further, to check the flow direction in HHHC, pressure measurement across the heater as well as temperature difference across hot and cold legs can be considered, as surface temperature measurement along the heater may not reflect the same. The scan time should be equal to or greater than the response time of all the sensors used in the system to capture flow transients sensibly.

As seen from some studies, if the cooler temperature decreases or the mass flow rate increases, there is a change in the threshold value with the former has a larger impact than the latter. Even the operating procedure also matters on stability threshold as discussed in [5, 19, 20].

Coupled natural circulation systems are seen to have various benefits like the single length of the primary loop can be reduced by introducing an intermediate NCL. If the heat source is too large for a single loop to transmit then parallel NCL can be thought off to equally distribute the heat source. When the heat sink is far out of reach, series NCL is a feasible option. More studies can be dedicated to CNCL as some of the authors have claimed that a CNCL is purely based on the least efficient loop and if any one of the loops is unstable, then the entire CNCL would be in the unstable zone. Such predictions can be tested with necessary experimental trials. Most of the studies in CNCL are devoted to nuclear application, which can be extended to solar thermal technology as the beam down concept is in limelight.

In line with the dearth of experimental studies in CNCL, a preliminary study undertaken with a series-coupled loop showed the feasibility of its functioning as a decay heat removal system (with atmosphere as the ultimate heat sink). Although the operating power range is low, with suitable high boiling point liquids, the range of operation and efficiency of CNCL can be enhanced.

To conclude, apart from the application of NCL in nuclear and solar thermal systems, there is a huge scope for its implementation, specifically in the thermal management of solar photovoltaics [113-115].

Acknowledgements

The authors gratefully acknowledge the financial support from SERB, DST under core research grant scheme (CRG/2019/004429).

Nomenclature

A	=	Flow area [m ²]
b	=	Value based on Re [-]
C_p	=	Specific heat [J/kg K]
C	=	Constant
D, d	=	Diameter [m]
f	=	Friction factor [-]
g	=	Gravitational acceleration [m/s ²]
Gr_m, Gr'	=	Modified Grashof number [-]
L	=	Length [m]
N_G	=	Geometry parameter [-]
Nu	=	Nusselt number [-]
p	=	Constant in friction factor equation [-]
P	=	Pressure [Pa]
Pr	=	Prandtl number [-]
Q	=	Core power [W]
Q_h	=	Total heat input rate [W]
Re	=	Reynolds number [-]
s	=	Super-critical
t	=	Time [s]
T	=	Temperature (K)
w, \dot{m}	=	Mass flow rate [kg/s]
Δz	=	Centerline deviation difference m]

Subscripts

amp	=	Amplitude
b	=	Bulk

i	=	Incline, inner
L	=	Laminar
or	=	Orifice
pc	=	Pseudo critical
R	=	Rolling condition
ss	=	Steady state
t	=	Total
T	=	Turbulent
v	=	Vertical
w	=	Wall

Greek letters

β	=	Orifice ratio (d_{or}/d_i) [-]
β_T	=	Thermal expansion coefficient [1/K]
δ	=	Effectiveness ratio [-]
Δ	=	Difference
ε	=	Effectiveness [-]
μ	=	Dynamic viscosity [Ns/m ²]
θ	=	Inclination angle [deg]
ρ	=	Density [kg/m ³]
ϕ_h	=	Phase of Instantaneous Nu_R

References:

[1] Vijayan, P. K., Nayak A. K. and Kumar. N, Single-phase, Two- phase and Supercritical Natural Circulation Systems. Woodhead Publishing, 2019.
<https://doi.org/10.1016/C2017-0-01142-4>

[2] Basu, D. N., Bhattacharyya, S. and P. K. Das. 2015. "A Review of Modern Advances in Analyses and Applications of Single-Phase Natural Circulation Loop in Nuclear Thermal Hydraulics." Nuclear Engineering and Design 280: 326–48.
<https://doi.org/10.1016/j.nucengdes.2014.09.011>

[3] Sarkar, M.K.S., Tilak, A. K. and Basu, D. N. 2014. "A State-of-the-Art Review of Recent Advances in Supercritical Natural Circulation Loops for Nuclear Applications." Annals of Nuclear Energy 73: 250–63.
<https://doi.org/10.1016/j.anucene.2014.06.035>

[4] Vijayan, P. K., A. K. Nayak, D. Saha, and M. R. Gartia. 2008. "Effect of Loop Diameter on the Steady State and Stability Behaviour of Single-Phase and Two-Phase Natural Circulation Loops." Science and Technology of Nuclear Installations 2008: 1-17.
<https://doi.org/10.1155/2008/672704>

[5] Elton, D.N., Arunachala, UC and Vijayan, PK, 2020. "Investigations on the dependence of the stability threshold on different operating procedures in a single-phase rectangular natural circulation loop." International Journal of Heat and Mass Transfer, 161, p.120264.
<https://doi.org/10.1016/j.ijheatmasstransfer.2020.120264>

[6] Vijayan, P. K. 2002. "Experimental Observations on the General Trends of the Steady State and Stability Behaviour of Single-Phase Natural Circulation Loops." Nuclear Engineering and Design 215 (1–2): 139–52.
[https://doi.org/10.1016/S0029-5493\(02\)00047-X](https://doi.org/10.1016/S0029-5493(02)00047-X)

[7] Kumar, N., Iyer, K.N., Doshi, J. B. and Vijayan, P.K. 2014. "Investigations on Single-Phase Natural Circulation Loop Dynamics. Part 2: Role of Wall Constitutive Laws." Progress in Nuclear Energy 75: 105–16.
<https://doi.org/10.1016/j.pnucene.2014.04.011>

[8] Meyer, Josua P., Leon Liebenberg, and Jonathan A. Olivier. "Measurement and evaluation of single-phase heat transfer and pressure drop inside enhanced tubes for transition flow." ASHRAE (American Society of Heating, Refrigerating and Air-Conditioning Engineers, Report nr: 1280-RP 204 (2008).

[9] Morcos, S. M., and A. E. Bergles. 1975. "Experimental Investigation of Combined Forced and Free Laminar Convection in Horizontal Tubes." Journal of Heat Transfer 97 (2): 212– 19. <https://doi.org/10.1115/1.3450343>

[10] Saha, Ritabrata, Swarnendu Sen, Saikat Mookherjee, Koushik Ghosh, Achintya Mukhopadhyay, and Dipankar Sanyal. 2015. "Experimental and Numerical Investigation of a Single-Phase Square Natural Circulation Loop." Journal of Heat Transfer 137 (12): 1–8.
<https://doi.org/10.1115/1.4030926>

[11] Naveen, Kumar, Kannan N. Iyer, J. B. Doshi, and P. K. Vijayan. 2015. "Investigations on Single- Phase Natural Circulation Loop Dynamics. Part 3: Role of Expansion Tank." Progress in Nuclear Energy 78: 65–79.
<https://doi.org/10.1016/j.pnucene.2014.08.007>

[12] Cheng, Haojie, Haiyan Lei, Long Zeng, and Chuanshan Dai. 2019. "Theoretical and Experimental Studies of Heat Transfer Characteristics of a Single-Phase Natural Circulation Mini-Loop with End Heat Exchangers." International Journal of Heat and Mass Transfer 128: 208–16.
<https://doi.org/10.1016/j.ijheatmasstransfer.2018.08.136>

[13] Cheng, H., Lei, H., Zeng, L., & Dai, C., 2019. "Experimental investigation of single-phase natural circulation in a mini-loop driven by heating and cooling fluids." Experimental Thermal and Fluid Science, 103, 182-190. <https://doi.org/10.1016/j.expthermflusci.2019.01.003>

[14] Seyyedi, S. M., N. Sahebi, A. S. Dogonchi, and M. Hashemi-Tilehnoee. 2019. "Numerical and Experimental Analysis of a Rectangular Single-Phase Natural Circulation Loop with Asymmetric Heater Position." International Journal of Heat and Mass Transfer 130: 1343–57.
<https://doi.org/10.1016/j.ijheatmasstransfer.2018.11.030>

[15] Krishnani, M. and Basu, D.N., 2017. "Computational stability appraisal of rectangular natural circulation loop: Effect of loop inclination." Annals of Nuclear Energy, 107, pp.17-30. <https://doi.org/10.1016/j.anucene.2017.04.012>

[16] Arunachala, U. C., A. C. Rajat, Shah, D. and Ujjawal, S. 2019. "Stability Improvement in Natural Circulation Loop Using Tesla Valve – an Experimental Investigation." International Journal of Mechanical and Production Engineer

ing Research and Development 9 (6): 13–24.
<https://doi.org/10.24247/ijmperddec20192>.

[17] Nie, Zesen, Bi, Qincheng, Wu, Di, and Wu, Jiangbo. "Experimental Study on the Natural Circulation System for Single-Phase Water." Proceedings of the ASME 2015 Power Conference. San Diego, California, USA. June 28– July 2, 2015. V001T12A004. ASME.
<https://doi.org/10.1115/POWER2015-49230>

[18] Misale, M., and M. Frogheri. 2001. "Stabilization of a Single-Phase Natural Circulation Loop by Pressure Drops." Experimental Thermal and Fluid Science 25 (5): 277– 282. [https://doi.org/10.1016/S0894-1777\(01\)00075-9](https://doi.org/10.1016/S0894-1777(01)00075-9).

[19] Elton, D.N., Arunachala, UC and Vijayan, PK, 2021. "Stability enhancement in large diameter rectangular natural circulation loops using flow restrictors." International Communications in Heat and Mass Transfer, 126, p.105412.
<https://doi.org/10.1016/j.icheatmasstransfer.2021.105412>

[20] Elton, D. N., Arunachala, U. C. and Rajat, A. C. (Article in press), "Influence of Orifice in Entropy Generation and Exergy Analysis under transient condition for Large Diameter Natural Circulation Loops", International journal of exergy.

[21] Misale, M. 2016. "Experimental Study on the Influence of Power Steps on the Thermohydraulic Behavior of a Natural Circulation Loop." International Journal of Heat and Mass Transfer 99: 782– 91.
<https://doi.org/10.1016/j.ijheatmasstransfer.2016.04.036>.

[22] Misale, M., P. Garibaldi, L. Tarozzi, and G. S. Barozzi. 2011. "Influence of Thermal Boundary Conditions on the Dynamic Behaviour of a Rectangular Single-Phase Natural Circulation Loop." International Journal of Heat and Fluid Flow 32 (2): 413–23.
<https://doi.org/10.1016/j.ijheatfluidflow.2010.12.003>.

[23] Likhmanets, I. and Baliga, B.R.R., 2019. "Experimental investigation of steady and transient operations of a single-phase closed-loop vertical thermosyphon." International Journal of Thermal Sciences, 145, p.105988.
<https://doi.org/10.1016/j.ijthermalsci.2019.105988>

[24] Huang, C.S., Yu, C.W., Chen, R.H., Tzeng, C.T. and Lai, C.M., 2019. "Experimental observation of natural convection heat transfer performance of a rectangular thermosyphon." Energies, 12(9), p.1702. <https://doi.org/10.3390/en12091702>

[25] Yun, E., Jeon, B.G. and Park, H.S., 2020. "Experimental study on a single-phase natural circulation loop and its steady-state solution." Applied Thermal Engineering, p.115190.
<https://doi.org/10.1016/j.applthermaleng.2020.115190>

[26] Zhu, Zhiqiang, Xiabin Cao, Changqi Yan, and Chunping Tian. "Local Single-Phase Heat Transfer Research of Natural Circulation in Narrow Rectangular Channel." In International Conference on Nuclear Engineering, vol. 57878, p. V009T15A014. American Society of Mechanical Engineers, 2017. <https://doi.org/10.1115/ICONE25-66542>

[27] Wang, Chang, Xiaohui Li, Hao Wang, and Puzhen Gao. 2014. "Experimental Study on Single- Phase Heat Transfer of Natural Circulation in Circular Pipe under Rolling Motion Condition." Nuclear Engineering and Design 273: 497–504. <https://doi.org/10.1016/j.nucengdes.2014.03.045>.

[28]. Yang, Ruichang, Ruolei Liu, Yong Zhong, and Tao Liu. 2006. "Experimental Study on Convective Heat Transfer of Water Flow in a Heated Tube under Natural Circulation." Nuclear Engineering and Design 236 (18): 1902–8.
<https://doi.org/10.1016/j.nucengdes.2006.01.013>.

[29] Tian, Wangsheng, Xiabin Cao, Changqi Yan, and Zhenxing Wu. 2017. "Experimental Study of Single-Phase Natural Circulation Heat Transfer in a Narrow, Vertical, Rectangular Channel under Rolling Motion Conditions." International Journal of Heat and Mass Transfer 107: 592–606.
<https://doi.org/10.1016/j.ijheatmasstransfer.2016.10.094>.

[30] Incropera, Frank P.; DeWitt, David P. (2000). Fundamentals of Heat and Mass Transfer (4th ed.). New York: Wiley. p. 493. ISBN 978-0-471-30460-9.

[31] Tian, Chunping, Ming Yan, Jianjun Wang, Xiabin Cao, Changqi Yan, and Shengzhi Yu. 2017. "Experimental Investigation of Flow and Heat Transfer for Natural Circulation Flow in an Inclined Narrow Rectangular Channel." Progress in Nuclear Energy 98: 266–76.
<https://doi.org/10.1016/j.pnucene.2017.04.004>.

[32] Shah, Ramesh K., and Alexander Louis London. Laminar flow forced convection in ducts: a source book for compact heat exchanger analytical data. Academic press, 2014.

[33] Steinke, Mark E., and Satish G. Kandlikar. 2006. "Single-Phase Liquid Friction Factors in Microchannels." International Journal of Thermal Sciences 45 (11): 1073–83.
<https://doi.org/10.1016/j.ijthermalsci.2006.01.016>.

[34] Blasius H. 1913. "The Law of Similarity for Frictions in Liquids," Notices of Research in the Field of Engineering." Notices of Research in the Field of Engineering 131: 1–41.
<https://doi.org/10.1007/978-3-662-02239-9>.

[35] Sadatomi, M., Y. Sato, and S. Saruwatari. 1982. "Two-Phase Flow in Vertical Noncircular Channels." International Journal of Multiphase Flow 8 (6): 641–55.
[https://doi.org/10.1016/0301-9322\(82\)90068-4](https://doi.org/10.1016/0301-9322(82)90068-4).

[36] Yu, Shengzhi, Jianjun Wang, Ming Yan, Changqi Yan, and Xiabin Cao. 2017. "Experimental and Numerical Study on Single-Phase Flow Characteristics of Natural Circulation System with Heated Narrow Rectangular Channel under Rolling Motion Condition." Annals of Nuclear Energy 103: 97– 113. <https://doi.org/10.1016/j.anucene.2017.01.008>.

[37] Sharma, Manish, P. K. Vijayan, D. S. Pilkhwal, and Yutaka Asako. 2014. "Natural Convective Flow and Heat Transfer Studies for Supercritical Water in a Rectangular

- Circulation Loop." *Nuclear Engineering and Design* 273: 304–20. <https://doi.org/10.1016/j.nucengdes.2014.04.001>.
- [38] Zhao, Dongliang, Christine Elizabeth Martini, Siyu Jiang, Yaoguang Ma, Yao Zhai, Gang Tan, Xiaobo Yin, and Ronggui Yang. 2017. "Development of a Single-Phase Thermosiphon for Cold Collection and Storage of Radiative Cooling." *Applied Energy* 205 (May): 1260–69. <https://doi.org/10.1016/j.apenergy.2017.08.057>.
- [39] Nayak, A K, M R Gartia, and P K Vijayan. 2008. "An Experimental Investigation of Single-Phase Natural Circulation Behavior in a Rectangular Loop with Al₂O₃ Nanofluids." *Experimental Thermal and Fluid Science* 33 (1): 184–189. <https://doi.org/10.1016/j.expthermflusci.2008.07.017>.
- [40] Xuan, Yimin, and Qiang Li. 2003. "Investigation on Convective Heat Transfer and Flow Features of Nanofluids." *Journal of Heat Transfer* 125 (1): 151–55. <https://doi.org/10.1115/1.1532008>.
- [41] Li, Qiang, and Yimin Xuan. 2002. "Convective Heat Transfer and Flow Characteristics of Cu- Water Nanofluid." *Science in China, Series E: Technological Sciences* 45 (4): 408–416. <https://doi.org/10.1360/02ye9047>.
- [42] He, Yurong, Yi Jin, Haisheng Chen, Yulong Ding, Daqiang Cang, and Huilin Lu. 2007. "Heat Transfer and Flow Behaviour of Aqueous Suspensions of TiO₂ Nanoparticles (Nanofluids) Flowing Upward through a Vertical Pipe." *International Journal of Heat and Mass Transfer* 50 (11–12): 2272–81. <https://doi.org/10.1016/j.ijheatmasstransfer.2006.10.024>.
- [43] Ho, C. J., Y. N. Chung, and Chi Ming Lai. 2014. "Thermal Performance of Al₂O₃/Water Nanofluid in a Natural Circulation Loop with a Mini-Channel Heat Sink and Heat Source." *Energy Conversion and Management* 87: 848–58. <https://doi.org/10.1016/j.enconman.2014.07.079>.
- [44] Doganay, Serkan, and Alpaslan Turgut. 2015. "Enhanced Effectiveness of Nanofluid Based Natural Circulation Mini Loop." *Applied Thermal Engineering* 75: 669–76. <https://doi.org/10.1016/j.applthermaleng.2014.10.083>.
- [45] Goudarzi, K., E. Shojaeizadeh, and F. Nejadi. 2014. "An Experimental Investigation on the Simultaneous Effect of CuO-H₂O Nanofluid and Receiver Helical Pipe on the Thermal Efficiency of a Cylindrical Solar Collector." *Applied Thermal Engineering* 73 (1): 1236–43. <https://doi.org/10.1016/j.applthermaleng.2014.07.067>.
- [46] Tiwari, Arun Kumar, Pradyumna Ghosh, and Jahar Sarkar. 2013. "Heat Transfer and Pressure Drop Characteristics of CeO₂/Water Nanofluid in Plate Heat Exchanger." *Applied Thermal Engineering* 57 (1–2): 24–32. <https://doi.org/10.1016/j.applthermaleng.2013.03.047>.
- [47] Mohammadian, Shahabeddin K., and Yuwen Zhang. 2014. "Analysis of Nanofluid Effects on Thermoelectric Cooling by Micro-Pin-Fin Heat Exchangers." *Applied Thermal Engineering* 70 (1): 282–90. <https://doi.org/10.1016/j.applthermaleng.2014.05.010>.
- [48] Ho, C. J., and W. C. Chen. 2013. "An Experimental Study on Thermal Performance of Al₂O₃/Water Nanofluid in a Mini channel Heat Sink." *Applied Thermal Engineering* 50 (1): 516–22. <https://doi.org/10.1016/j.applthermaleng.2012.07.037>.
- [49] Koca, Halil Dogacan, Serkan Doganay, and Alpaslan Turgut. 2017. "Thermal Characteristics and Performance of Ag-Water Nanofluid: Application to Natural Circulation Loops." *Energy Conversion and Management* 135: 9–20. <https://doi.org/10.1016/j.enconman.2016.12.058>.
- [50] Haddad, Zoubida, Hakan F. Oztop, Eiyad Abu-Nada, and Amina Mataoui. 2012. "A Review on Natural Convective Heat Transfer of Nanofluids." *Renewable and Sustainable Energy Reviews* 16 (7): 5363–78. <https://doi.org/10.1016/j.rser.2012.04.003>.
- [51] Taylor, Robert, Sylvain Coulombe, Todd Otanicar, Patrick Phelan, Andrey Gunawan, Wei Lv, Gary Rosengarten, Ravi Prasher, and Himanshu Tyagi. 2013. "Small Particles, Big Impacts: A Review of the Diverse Applications of Nanofluids." *Journal of Applied Physics* 113 (1). <https://doi.org/10.1063/1.4754271>.
- [52] Thomas, Shijo, and Choondal B. Sobhan. 2018. "Stability and Transient Performance of Vertical Heater Vertical Cooler Natural Circulation Loops with Metal Oxide Nanoparticle Suspensions." *Heat Transfer Engineering* 39 (10): 861–73. <https://doi.org/10.1080/01457632.2017.1338859>.
- [53] Vijayan, P. K., M. Sharma, and D. Saha. 2007. "Steady State and Stability Characteristics of Single-Phase Natural Circulation in a Rectangular Loop with Different Heater and Cooler Orientations." *Experimental Thermal and Fluid Science* 31 (8): 925–45. <https://doi.org/10.1016/j.expthermflusci.2006.10.003>.
- [54] Bejjam, R.B., Kiran Kumar, K. and Balasubramanian, K., 2019. "Experimental Studies on Nanofluid-Based Rectangular Natural Circulation Loop." *Journal of Thermal Science and Engineering Applications*, 11(4). <https://doi.org/10.1115/1.4043760>
- [55] Tlili, I., Seyyedi, S.M., Dogonchi, A.S., Hashemi-Tilehnoee, M. and Ganji, D.D., 2020. "Analysis of a single-phase natural circulation loop with hybrid-nanofluid." *International Communications in Heat and Mass Transfer*, 112, p.104498. <https://doi.org/10.1016/j.icheatmasstransfer.2020.104498>
- [56] Ho, C. J., Y. Z. Chen, Fong Jou Tu, and Chi Ming Lai. 2014. "Thermal Performance of Water- Based Suspensions of Phase Change Nanocapsules in a Natural Circulation Loop with a Mini- Channel Heat Sink and Heat Source." *Applied Thermal Engineering* 64 (1–2): 376–84. <https://doi.org/10.1016/j.applthermaleng.2013.12.051>.

- [57] Swapnalee, B. T., P. K. Vijayan, M. Sharma, and D. S. Pilkhwal. 2012. "Steady State Flow and Static Instability of Supercritical Natural Circulation Loops." *Nuclear Engineering and Design* 245: 99–112. <https://doi.org/10.1016/j.nucengdes.2012.01.002>.
- [58] Liu, Guangxu, Yanping Huang, Junfeng Wang, Fa Lv, and Laurence K.H. Leung. 2016. "Experiments on the Basic Behavior of Supercritical CO₂ Natural Circulation." *Nuclear Engineering and Design* 300: 376–83. <https://doi.org/10.1016/j.nucengdes.2016.01.021>.
- [59] Liu, Guangxu, Yanping Huang, Junfeng Wang, and Laurence H.K. Leung. 2016. "Heat Transfer of Supercritical Carbon Dioxide Flowing in a Rectangular Circulation Loop." *Applied Thermal Engineering* 98: 39–48. <https://doi.org/10.1016/j.applthermaleng.2015.11.110>.
- [60] Bishop, A. A., R. O. Sandberg, and L. S. Tong. Forced-convection heat transfer to water at near- critical temperatures and super-critical pressures. No. WCAP-5449; CONF-650603-1. Westinghouse Electric Corp., Pittsburgh, Pa. Atomic Power Div., 1964.
- [61] Krasnoshchekov, E. A., and V. S. Protopopov. "Heat transfer at super-critical region in flow of carbon dioxide and water in tubes." *Therm. Energy* 12 (1959): 26-30.
- [62] Swenson, H. S., J. R. Carver, and CR D. Kakarala. "Heat transfer to super-critical water in smooth- bore tubes." (1965): 477-483. <https://doi.org/10.1115/1.3689139>
- [63] Jackson, J. D. 2013. "Fluid Flow and Convective Heat Transfer to Fluids at Supercritical Pressure." *Nuclear Engineering and Design* 264: 24–40. <https://doi.org/10.1016/j.nucengdes.2012.09.040>.
- [64] Liu, Guangxu, Yanping Huang, Junfeng Wang, Fa Lv, and Shenghui Liu. 2017. "Experimental Research and Theoretical Analysis of Flow Instability in Supercritical Carbon Dioxide Natural Circulation Loop." *Applied Energy* 205 (March): 813–21. <https://doi.org/10.1016/j.apenergy.2017.08.132>.
- [65] Liu, Guangxu, Yanping Huang, Junfeng Wang, and Fa Lv. 2015. "Effect of Buoyancy and Flow Acceleration on Heat Transfer of Supercritical CO₂ in Natural Circulation Loop." *International Journal of Heat and Mass Transfer* 91: 640– 46. <https://doi.org/10.1016/j.ijheatmasstransfer.2015.08.009>.
- [66] Liu, G., Huang, Y. and Wang, J., 2019. "A new theoretical model of steady-state characteristics of super-critical carbon dioxide natural circulation." *Energy*, 189, p.116323. <https://doi.org/10.1016/j.energy.2019.116323>
- [67] Lomperski, S., D. Cho, R. Jain, and M. L. Corradini. "Stability of a natural circulation loop with a fluid heated through the thermodynamic pseudo-critical point." In *Proceedings of the 2004 international congress on advances in nuclear power plants-ICAPP'04*. 2004.
- [68] Sharma, M., Vijayan, P.K., Pilkhwal, D.S. and Asako, Y., 2013." Steady state and stability characteristics of natural circulation loops operating with carbon dioxide at super-critical pressures for open and closed loop boundary conditions." *Nuclear Engineering and Design*, 265, pp.737-754. <https://doi.org/10.1016/j.nucengdes.2013.07.023>
- [69] Chen, Lin, Xin Rong Zhang, and Bi Li Deng. 2016. "Near-Critical Natural Circulation Flows Inside an Experimental Loop: Stability Map and Heat Transfer." *Heat Transfer Engineering* 37 (3– 4): 302–13. <https://doi.org/10.1080/01457632.2015.1052680>.
- [70] Zhang, Lei, Vijay Chatoorgoon, and Robert Derksen. "Experimental Flow Instability Study of a Natural Circulation Loop with Supercritical CO₂." In *International Conference Pacific Basin Nuclear Conference*, pp. 121-141. Springer, Singapore, 2016. <https://doi.org/10.1007/978-981-10-2314-9>.
- [71] Sadhu, Sayan, Maddali Ramgopal, and Souvik Bhattacharyya. 2018. "Experimental Studies on an Air-Cooled Natural Circulation Loop Based on Supercritical Carbon Dioxide – Part A: Steady State Operation." *Applied Thermal Engineering* 133: 809–18. <https://doi.org/10.1016/j.applthermaleng.2017.10.017>.
- [72] L. Chen, X.-R. Zhang, S. Cao, H. Bai. 2012. "Study of trans-critical CO₂ natural convective flow with unsteady heat input and its implications on system control." *Int. J. Heat Mass Transfer* 55 (2012) 7119– 7132. <https://doi.org/10.1016/j.ijheatmasstransfer.2012.07.027>.
- [73] A.K. Yadav, M. Ram Gopal, S. Bhattacharyya.2012. "CO₂ based natural circulation loops: new correlations for friction and heat transfer." *Int. J. Heat Mass Transfer* 55 (2012) 4621– 4630. <https://doi.org/10.1016/j.ijheatmasstransfer.2012.04.019>.
- [74] Sadhu, Sayan, Maddali Ramgopal, and Souvik Bhattacharyya. 2018. "Experimental Studies on an Air-Cooled Natural Circulation Loop Based on Supercritical Carbon Dioxide – Part B: Transient Operation." *Applied Thermal Engineering* 133: 819–27. <https://doi.org/10.1016/j.applthermaleng.2017.10.016>.
- [75] Deng, B., Chen, L., Zhang, X. and Jin, L., 2019. "The flow transition characteristics of super-critical CO₂ based closed natural circulation loop (NCL) system." *Annals of Nuclear Energy*, 132, pp.134-148. <https://doi.org/10.1016/j.anucene.2019.04.032>
- [76] Yadav, Ajay Kumar, Maddali Ramgopal, and Souvik Bhattacharyya. 2017. "Transient Analysis of Subcritical/Supercritical Carbon Dioxide Based Natural Circulation Loop with End Heat Exchangers: Experimental Study." *Heat and Mass Transfer/Waerme-Und Stoffuebertragung* 53 (9): 2951–60. <https://doi.org/10.1007/s00231-017-2038-z>.

- [77] Kumar K K, Ramgopal M. 2009. "Carbon dioxide as secondary fluid in natural circulation loops." Proc IMechE, Part E: J Process Mech Eng 223:189–194. <https://doi.org/10.1243/09544089JPME242>
- [78] Thippeswamy, L.R. and Yadav, A.K., 2020. "Heat transfer enhancement using CO₂ in a natural circulation loop." Scientific reports, 10(1), pp.1-10. <https://doi.org/10.1038/s41598-020-58432-6>
- [79] Naphade, P., A. Borgohain, R. Thundil Karuppa Raj, and N. K. Maheshwari. 2013. "Experimental and CFD Study on Natural Circulation Phenomenon in Lead Bismuth Eutectic Loop." Procedia Engineering 64: 936–45. <https://doi.org/10.1016/j.proeng.2013.09.170>.
- [80] Borgohain, A., N. K. Maheshwari, and P. K. Vijayan. 2016. "Natural Circulation Experiments in a Non-Uniform Diameter Lead Bismuth Loop and Validation of LeBENC Code." Progress in Nuclear Energy 91: 68–82. <https://doi.org/10.1016/j.pnucene.2016.03.005>.
- [81] Shin, Yong Hoon, Jaehyun Cho, Jueun Lee, Heejae Ju, Sungjune Sohn, Yeji Kim, Hyunub Noh, and Il Soon Hwang. 2017. "Experimental Studies and Computational Benchmark on Heavy Liquid Metal Natural Circulation in a Full Height-Scale Test Loop for Small Modular Reactors." Nuclear Engineering and Design 316: 26–37. <https://doi.org/10.1016/j.nucengdes.2017.03.001>.
- [82] Ryu, Kyung Ha, Byoung Min Ban, Tae Hyun Lee, Jeonghyeon Lee, Sang Huk Lee, Jae Hyun Cho, Sung ho Ko, and Ji Hyun Kim. 2018. "Natural Circulation Characteristics under Various Conditions on Heavy Liquid Metal Test Loop." International Journal of Thermal Sciences 132: 316–21. <https://doi.org/10.1016/j.ijthermalsci.2018.06.015>.
- [83] Srivastava, A. K., Jayaraj Y. Kudariyawar, A. Borgohain, S. S. Jana, N. K. Maheshwari, and P. K. Vijayan. 2016. "Experimental and Theoretical Studies on the Natural Circulation Behavior of Molten Salt Loop." Applied Thermal Engineering 98: 513–21. <https://doi.org/10.1016/j.applthermaleng.2015.12.065>.
- [84] Kudariyawar, Jayaraj Yallappa, Abhishek Kumar Srivastava, Abhijeet Mohan Vaidya, Naresh Kumar Maheshwari, and Polepalle Satyamurthy. 2016. "Computational and Experimental Investigation of Steady State and Transient Characteristics of Molten Salt Natural Circulation Loop." Applied Thermal Engineering 99: 560–71. <https://doi.org/10.1016/j.applthermaleng.2015.12.114>.
- [85] Shin, Yukyung, Seok Bin Seo, In Guk Kim, and In Cheol Bang. 2016. "Natural Circulation with DOWTHERM RP and Its MARS Code Implementation for Molten Salt-Cooled Reactors." International Journal of Energy Research 40 (8): 1122–33. <https://doi.org/10.1002/er.3512>.
- [86] Scarlat, R.O., Laufer, M.R., Blandford, E.D., Zweibaum, N., Krumwiede, D.L., Cisneros, A.T., Andreades, C., Forsberg, C.W., Greenspan, E., Hu, L.W. and Peterson, P.F., 2014. "Design and licensing strategies for the fluoride-salt-cooled, high-temperature reactor (FHR) technology." Progress in Nuclear Energy, 77: 406–420. <https://doi.org/10.1016/j.pnucene.2014.07.002>
- [87] Britsch, K., Anderson, M., Brooks, P. and Sridharan, K., 2019. "Natural circulation FLiBe loop overview." International Journal of Heat and Mass Transfer 134: 970–983. <https://doi.org/10.1016/j.ijheatmasstransfer.2018.12.180>
- [88] Cataldo, Filippo, and John Richard Thome. 2018. "Experimental Performance of a Completely Passive Thermosyphon Cooling System Rejecting Heat by Natural Convection Using the Working Fluids R1234ze, R1234yf, and R134a." Journal of Electronic Packaging, Transactions of the ASME 140 (2): 1–11. <https://doi.org/10.1115/1.4039706>.
- [89] Rahmani, Ahmed, Abdelouahab Boutriaa, and Amar Hadeif. 2015. "An Experimental Approach to Improve the Basin Type Solar Still Using an Integrated Natural Circulation Loop." Energy Conversion and Management 93: 298–308. <https://doi.org/10.1016/j.enconman.2015.01.026>.
- [90] Zvirin, Y., P. R. Jeuck, C. W. Sullivan, and R. B. Duffey. 1981. "Experimental and Analytical Investigation of a Natural Circulation System with Parallel Loops." Journal of Heat Transfer 103 (4): 645–52. <https://doi.org/10.1115/1.3244521>.
- [91] Davis, S.H. and Roppo, M.N., 1987. "Coupled Lorenz oscillators. Physica D: Nonlinear Phenomena." 24(1-3): 226–242. [https://doi.org/10.1016/0167-2789\(87\)90077-7](https://doi.org/10.1016/0167-2789(87)90077-7)
- [92] Salazar, O., Sen, M. and Ramos, E. 1988. "Flow in Conjugate Natural Circulation Loops." Journal of Thermophysics and Heat Transfer 2 (2): 180–83. <https://doi.org/10.2514/3.83>.
- [93] Ehrhard, P., Ch. Marcher, and U. Müller. 1989. "Dynamical Behavior of Natural Convection in a Double-Loop System." Experimental Heat Transfer 2 (1): 13–26. <https://doi.org/10.1080/08916158908946351>.
- [94] Satoh, A., K. Okamoto, and H. Madarame. 1998. "Instability of Single-Phase Natural Circulation under Double Loop System." Chaos, Solitons and Fractals 9 (9): 1575–85. [https://doi.org/10.1016/S0960-0779\(97\)00117-3](https://doi.org/10.1016/S0960-0779(97)00117-3).
- [95] Satou, Akira, Haruki Madarame, and Koji Okamoto. 2001. "Unstable Behavior of Single-Phase Natural Circulation under Closed Loop with Connecting Tube." Experimental Thermal and Fluid Science 25 (6): 429–35. [https://doi.org/10.1016/S0894-1777\(01\)00092-9](https://doi.org/10.1016/S0894-1777(01)00092-9).
- [96] Marchitto, Annalisa, and Mario Misale. 2018. "Experiments on Parallel Connected Loops in Single Phase Natural Circulation: Preliminary Results." Mathematical Modelling of Engineering Problems 5 (3): 61–167. <https://doi.org/10.18280/mmep.050305>.
- [97] Dass, Akhil, and Sateesh Gedupudi. 2019. "1-D Semi-Analytical Modeling and Parametric Study of a Single Phase

Rectangular Coupled Natural Circulation Loop." *Chemical Engineering Science* 207: 105–29.
<https://doi.org/10.1016/j.ces.2019.05.050>.

[98] Cheng, Lap Y., Hans Ludewig, and Jae Jo. 2006. "Emergency Decay Heat Removal in a GEN- IV Gas-Cooled Fast Reactor." *International Conference on Nuclear Engineering, Proceedings, ICONE 2006*: 1–10.
<https://doi.org/10.1115/ICONE14-89681>.

[99] Cheng, Lap Yan, and Thomas Y.C. Wei. 2009. "Decay Heat Removal in GEN IV Gas-Cooled Fast Reactors." *Science and Technology of Nuclear Installations 2009*.
<https://doi.org/10.1155/2009/797461>.

[100] Krepper, Eckhard, and Matthias Beyer. 2010. "Experimental and Numerical Investigations of Natural Circulation Phenomena in Passive Safety Systems for Decay Heat Removal in Large Pools." *Nuclear Engineering and Design* 240 (10): 3170–77.
<https://doi.org/10.1016/j.nucengdes.2010.05.050>.

[101] Damiani, Lorenzo, and Alessandro Pini Prato. 2015. "Simulation Model of a Passive Decay Heat Removal System for Lead-Cooled Fast Reactors." *Journal of Engineering for Gas Turbines and Power* 137 (3): 1–8.
<https://doi.org/10.1115/1.4028459>.

[102] Damiani, Lorenzo, Pietro Giribone, Roberto Revetria, and Alessandro Pini Prato. 2015. "A Passive Decay Heat Removal System for the Lead Cooled Fast Reactor Demonstrator 'Alfred.'" *Progress in Nuclear Energy* 83: 294–304. <https://doi.org/10.1016/j.pnucene.2015.04.005>

[103] Chung, Young Jong, Hyun Sik Park, Won Jae Lee, and Keng Koo Kim. 2015. "Heat Transfer in a Cooling Water Pool with Tube Bundles under Natural Circulation." *Annals of Nuclear Energy* 77: 402–7.
<https://doi.org/10.1016/j.anucene.2014.11.043>.

[104] Ono, Ayako, Hideki Kamide, Jun Kobayashi, Norihiro Doda, and Osamu Watanabe. 2016. "An Experimental Study on Natural Circulation Decay Heat Removal System for a Loop Type Fast Reactor." *Journal of Nuclear Science and Technology* 53 (9): 1385–96.
<https://doi.org/10.1080/00223131.2015.1121844>.

[105] Lv, Xing, Minjun Peng, Xiao Yuan, and Genglei Xia. 2016. "Design and Analysis of a New Passive Residual Heat Removal System." *Nuclear Engineering and Design* 303: 192–202. <https://doi.org/10.1016/j.nucengdes.2016.03.020>.

[106] Pal, Eshita, Mukesh Kumar, Arun K. Nayak, and Jyeshtharaj B. Joshi. 2016. "Experimental and CFD Simulations of Fluid Flow and Temperature Distribution in a Natural Circulation Driven Passive Moderator Cooling System of an Advanced Nuclear Reactor." *Chemical Engineering Science* 155: 45–64.
<https://doi.org/10.1016/j.ces.2016.07.037>.

[107] Kumar, Mukesh, A. K. Nayak, and J. B. Joshi. 2017.

"Investigations of Natural Convection and Circulation in Passive Moderator Cooling System of an Advanced Reactor in a Scaled Test Facility." *Nuclear Engineering and Design* 322: 55–67. <https://doi.org/10.1016/j.nucengdes.2017.06.018>.

[108] Kumar, Sunil, P. K. Vijayan, Umasankari Kannan, Manish Sharma, and D. S. Pilkhwal. 2017. "Experimental and Computational Simulation of Thermal Stratification in Large Pools with Immersed Condenser." *Applied Thermal Engineering* 113: 345–61.
<https://doi.org/10.1016/j.applthermaleng.2016.10.175>.

[109] Vijayan, P K, Ramakrishna, T., Borgohain, A., Lingade, B.M., Mahender, D., 2018a. "A diverse passive fuel cooling system for advanced high temperature reactors." *The 6th International Conference on Nuclear and Renewable energy resources (NURER2018)*, Jeju, Korea, 30 September- October 2018.

[110] Vijayan, P.K., Sinha, S.K., Singh, R.K., Kumar, A., Vishnoi, A.K., Kaushik, A., et al., 2018b. "Conceptual design of a mini solar thermal power plant." *The 6th International Conference on Nuclear and Renewable Energy Resources (NURER2018)*, Jeju, Korea, 30 September- October 2018.

[111] Thalange, Vinayak C., Eshita Pal, Nitin Minocha, Arun K. Nayak, Sanjay M. Mahajani, Sudhir V. Panse, and Jyeshtharaj B. Joshi. 2018. "Thermal Hydraulics of Natural Circulation Loop in Beam- down Solar Power Tower." *Energy* 159: 1088–1101.
<https://doi.org/10.1016/j.energy.2018.06.156>.

[112] Elton, D.N., Arunachala, U.C. and Dolfred, V.F., 2020. Efficacy of air heat exchanger based decay heat removal system through passive mode: A numerical study. *Materials Today: Proceedings* 28: 2286-2294.
<https://doi.org/10.1016/j.matpr.2020.04.566>

[113] Farzaneh Ghasemzadeh, Mahdi Esmaeilzadeh and Mostafa Esmaeili Shayan. 2020. "Photovoltaic Temperature Challenges and Bismuthene Monolayer Properties". *International journal of Smart Grid* 4(4): 190-195.
<https://www.ijsmartgrid.org/index.php/ijsmartgridnew/article/view/131/pdf>

[114] Grazia Todeschini, Han Huang, Noel Bristow, Tudur Wyn David and Jeff Kettle. 2020. "A Novel Computational Model for Organic PV Cells and Modules". *International journal of Smart Grid* 4(4): 157-163.
<https://www.ijsmartgrid.org/index.php/ijsmartgridnew/article/view/127/pdf>

[115] Kenneth Okedu, Abdulaziz Salem AlSenaidi, Imaduddin Al Hajri, Issa Al Rashdi, Waleed Al Salmani. 2020. "Real Time Dynamic Analysis of Solar PV Integration for Energy Optimization". *International journal of Smart Grid* 4(2): 68-79.
<https://www.ijsmartgrid.org/index.php/ijsmartgridnew/article/view/14/pdf>